PNEUMATIC ERGONOMIC CRUTCHES

BY

CHENZHANG XIAO

THESIS

Submitted in partial fulfillment of the requirements
for the degree of Master of Science in Mechanical Engineering
in the Graduate College of the
University of Illinois at Urbana-Champaign, 2017

Urbana, Illinois

Adviser:

Professor Elizabeth T. Hsiao-Wecksler

ABSTRACT

Long-term crutch users utilize Lofstrand crutches for locomotion commonly using swing-through or reciprocal gait patterns. Repetitive high forces, hyperextension and ulnar deviation of the wrist, and excessive palmar pressure compressing the median nerve associated with crutch walking have reported to cause discomfort, joint pain, wrist strain, carpal tunnel syndrome and other serious injuries. To address these issues, we developed the pneumatic ergonomic crutches (PEC) that consisted of a pneumatic sleeve orthosis, an energy harvesting system and an energy storage system. The pneumatic sleeve orthosis utilized a soft pneumatic actuator, called fiber-reinforced elastomeric enclosure, coiled around the forearm and secured to the cuff. In the first study, sleeve orthosis performance was examined. Human subject testing indicated significantly improved wrist posture, increased loading sharing to the cuff, reduced and redirected palmar pressure while using the orthosis. In the second study, the fully-developed PEC was presented. The PEC utilized an energy harvesting piston pump to collect pneumatic energy during crutch gait. The collected pneumatic energy was stored into a pneumatic elastomeric accumulator (PEA) inside the crutch shaft, which can be used to inflate the sleeve orthosis to make a self-contained crutch system. We optimized dimensions and specifications of the piston pump and the PEA to minimize the number of gait cycles used to charge the PEA to a target pressure that can be used to fully charge the sleeve orthosis. Bench-top testing was conducted on the PEC and demonstrated the ability of charging the sleeve orthosis using air stored in the PEA after 38 gait cycles. Protocols for future human subject testing to evaluate the system performance of the PEC were also presented.

To my family, friends and mentor

ACKNOWLEDGEMENTS

I would like to thank my advisor, Elizabeth Hsiao-Wecksler, for giving me the opportunity to work in the Human Dynamics and Controls Lab (HDCL) and for her kind guidance, generous support and profound inspirations throughout various stages of this project.

I would also like to thank every former and present members in the Human Dynamics and Controls Lab for their support and help during the past a few years. In particular, I would like to thank my graduate mentors during my undergraduate years, Deen Fraooq and Mazharul Islam, and my colleagues during my graduate years who provided their insights in various aspects (Ziming Wang, Carrie Liang, Alan Gaglio, Matt Pretrucci, Yinan Pei, Leo Song, Cathy Shih, Nick Thompson and Maria Fox). I would also like to thank undergraduate students who have been working with me, Ye Lwin Oo, David Lin and Prateek Garag. In addition, I need to thank Prof. Girish Krishnan and his graduate student Gaurav Singh at the University of Illinois, who have provided their expertise in the soft pneumatic actuator through the design stage of the project. Moreover, I need to thank Prof. Brooke Slavens and her students and staff Omid Jahanian, Alyssa Schnorenberg and Justin Riebe in the Mobility Lab in the University of Wisconsin-Milwaukee, who have worked with me on the human subject testing, helped with data processing and provided their expertise and proficient experience in crutch gait biomechanics. Additionally, I would like to thank the Center of Compact and Efficient Fluid Power (CCEFP) and the National Science Foundation (NSF) for their funding on this project (#0540834).

Last but not least, I would like to thank my parents, Lili Wang and Meixin Xiao, for their unconditional love, guidance and support during all these years to allow me be able to pursuit my dream in a country far away from our home land.

TABLE OF CONTENTS

CHAPTER 1: LITERATURE REVIEW

1.1 LONG-TERM CRUTCH USERS

As of the year of 2000, there were over 6.8 million Americans who used assistive devices to help them with mobility, including 6.1 million users walking with canes, crutches, and walkers [1]. The number of crutch users were estimated to be 566,000. Among all crutch users, 6% of them are under 18, 66% of them are between 16 and 64, and 28% are over 65 [1]. The top four conditions associated with the use of crutches among adults included: osteoarthritis, orthopedic impairments of the lower extremity, absence or loss of lower extremity, and chronic injuries or late effects of injuries [1].

1.2 CRUTCH DESIGNS AND GAIT PATTERNS

There are three types of basic crutches: axillary, forearm, and platform crutches. The axillary, or underarm, crutch is mostly recommended for short-term usage (Figure 1.1a) [2]. It has an axillary bar under the armpit, a handgrip and two vertical supports jointed at the distal end to form a single-leg support. The body weight is supported through the wrist. The forearm crutch, or Lofstrand crutch, is recommended for long-term use (Figure 1.1b) [3]. It has a single metal tube forming the crutch shaft, a crutch handle, and a crutch cuff. The shaft is angled 15 degrees above the crutch handle to form a crutch neck, with a cuff attached to the top of that. The user dons the crutch cuff and holds the crutch handle. Body weight is mainly supported through the wrist during crutch walking. The cuff can be rotating around the crutch neck, allowing the user to perform daily activities without taking off the crutch. The weight of the Lofstrand crutch is generally lighter than that of axillary crutch. The platform crutch is recommended for crutch users who have elbow contractures or whose wrists and hands are weak and painful (Figure 1.1c) [2]. It has a single metal tube forming the crutch shaft and a horizontal plate to rest the forearm,

and a vertical handle. A strap may additionally be used to secure the forearm in the horizontal plate. Body weight is supported through the medial side of the forearm when walking with platform crutches.

Five types of crutch gait are commonly used by crutch users: 2-point alternative crutch gait, 3-point alternative crutch gait, 4-point alternative crutch gait, and swing-through crutch gait (Figure 1.2) [4]. Different crutch gait patterns are adopted based on different levels of strength in the crutch users' lower extremities. 2-point alternative crutch gait, also known as reciprocal gait, most closely resembles normal walking and requires a moderate amount of support from the lower extremities. The sequence of this gait is right crutch and left foot; left crutch and right foot. For 3-point alternative gait, two crutches and the weaker leg move forward simultaneously, then the strong leg is swung forward while placing most of the body weight on the arms. 4-point alternative crutch gait is slowest of all crutch gaits, and requires a larger amount of support from the lower extremities. The sequence of 4-point crutch gait is for example: right crutch, left foot, left crutch, right foot. Swing-through gait is the fastest and most demanding of all crutch gaits. People with low strength in both legs are recommended to use this gait pattern for locomotion. In this process, they first advance both crutches forward, lift both legs off the ground, and then swing forward the legs landing in advance of the crutches. Reciprocal and swing-through crutch gait are most commonly used when walking with Lofstrand crutches [5].

1.3 BIOMECHANICS OF CRUTCH-ASSISTED GAIT

Crutch-assisted gait reduces the amount of load on the lower extremities during locomotion. The kinematics and kinetics of the upper extremities have been studied to further understand the effect of crutch-assisted gait onto the upper extremities [6-13].

Upper extremity kinematics have been studied during crutch-assisted swing-through and reciprocal gait [9-11,13]. Shoulder, elbow and wrist joints experience significantly higher range of motion in swing-through gait than in reciprocal gait [13]. Repetitive hyperextension and prolonged ulnar deviation

of the wrist have been observed during both crutch gaits [9-11]. In swing-through gait, hyperextension of the wrist ranging from 30-40 degrees during the body stance phase and up to 60 degrees during the crutch stance phase have been observed. The wrist extension angles were smaller during reciprocal gait. A clear cyclic wrist extension movement pattern, with a range of motion of 10-20 degrees, have also been identified in both gait patterns. Moreover, consistent ulnar deviation ranges from around 10-20 degrees were also observed in both gait patterns.

The joint kinetics have also been studied using instrumented crutches and upper extremity inverse-dynamics models [9-12]. Shoulder, elbow and wrist joints unilaterally experience forces ranging from 5% of body weight to more than 50% of body weight during crutch gait along with high peak force during crutch stance phase and rapidly increasing impulse force during crutch strike. A wrist joint can experience up to 25% of body weight in reciprocal gait, due to existence of the double support phase in this gait pattern. Swing-through crutch gait is more biomechanically taxing. The peak wrist force can reach more than 50% of the body weight during in the crutch stance phase, when the user pushes on both crutches and swings the body forward. The joint forces also increase rapidly from 0 to peak magnitude within 200 ms after initial crutch strike.

1.4 INJURIES ASSOCIATED WITH CRUTCH WALKING

Crutch users have reported pain and injuries in one or more joints in their upper extremities due to long-term crutch use [14]. People using assistive devices for locomotion are more likely to develop carpal tunnel syndrome (CTS) (Figure 1.3) [15-17], which has symptoms involving pain in the hand and arm with numbness and tingling [18]. Conditions that develop CTS overlap with kinematic and kinetic conditions of the wrist during crutch walking. Repetitive wrist flexion-extension, radial-ulnar deviation, as well as external force applied in the carpal tunnel of the palm compressing the median nerve, which are observed in crutch gait, have been shown to increase the median nerve pressure temporarily [19-23].

Such increase is highly associated with the onset and development of CTS [22,23]. A strong correlation was also found between the hand holding the crutch and the hand in which CTS developed in long-term crutch users [15-16]. The treatment of CTS involves surgical solutions to release the median nerve pressure and preventive measures to restrict wrist movement, keep the wrist in a neutral position, and reduce palmar pressure [17, 20, 24]. However, if CTS is not prevented in its onset, post treatments would have small effect in the long term. In addition, preventative measures are beneficial during the activities since symptoms associated with CTS may not appear until several hours after aggressive use of the hand and wrist without giving any alert [25].

Joint deformity and other neuropathies are prevalent among crutch users [14, 25-28]. These injuries are also caused by improper wrist posture, excessive pressure in the palm, as well as a large impulse force and high peak force acting at the wrist joint.

1.5 CURRENT SOLUTIONS

Engineers and designers have investigated into different designs of crutches to reduce forces experienced by the user's wrist. Smart Crutch (Smart Crutch, Inc., CA) is a combination of a Lofstrand and platform crutch (Figure 1.1d). It has an adjustable forearm platform that can be angled from 0 to 60 degrees about the horizontal plane such that user's body weight is supported and shared by both the wrist and the medial side of the forearm. However, no biomechanical study has been conducted on this design. The biomechanics of the crutch gait using an angle forearm plate is still unknown. People have also designed and commercialized crutches with additional shock absorption features by integrating a spring into the crutch shaft (Ergobaum forearm crutches, Ergoactives Orthopedic Device Company, Hallandale Beach, FL) (Figure 1.1e). The spring-loaded components provide shock absorption and help with crutch propulsion during crutch gait. The spring-loaded crutches absorb kinetic energy during crutch strike and transfer it to elastic energy of the spring. During the end of the crutch stance phase, the stored

elastic energy in the spring then transfers back to kinetic energy to provide a propulsion force as the crutch tip leaves the ground. Studies have shown a significantly increased mechanical efficiency when walking with spring-loaded crutches [29]. The total energy expenditure can also be reduced with an optimized spring coefficient [30-32]. Researchers compared the resultant ground reaction force (GRF) in spring-loaded crutches and standard crutches [30,33]. The study indicated a significantly decreased rate of rise in the resultant GRF during the crutch stance phase and significantly reduce magnitude of resultant GRF at 50, 100, and 200 ms. However, a slight increase in the peak GRF was observed, due to a lack of a damping component (Figure 1.4). Moreover, subjects have also reported improved endurance and comfort with the spring-loaded crutches [34].

People have also investigated into designing attachments or accessories to the crutches to help crutch users. A wider crutch grip was expected to reduce palmar pressure; however, it produced a similar pressure distribution as regular grip [35] (Figure 1.5a). A universal ergonomic crutch grip was designed to increase the contact area of the palm and to guide the user to form a better wrist posture [36] (Figure 1.5b). Increasing contact area may effectively reduce the palmar pressure and guiding the hand posture may also result in a more neutral wrist position. However, no scientific study has been conducted to validate the effect of this ergonomic crutch handle. A design of an elastic crutch tip that can be compressed during crutch strike was attached in a pair of commercially available crutches (B+M crutches, Mobility Designed, LLC, Kansas City, MO), which may have similar shock absorption effect as the spring-loaded crutches (Figure 1.5c) [69]. However, no scientific study has been conducted to validate such effect of the elastic crutch tip as well. A passive wrist orthosis was developed to improve wrist posture and redirect palmar pressure (Figure 1.5d) [37]. The orthosis was composed of a 3D printed curved structure that can be secured to the crutch handle and the crutch neck, and a taut nylon strap providing wrist support and restricting wrist extension. Human subject testing was conducted to evaluate the effectiveness of the device in terms of improving wrist posture and redirecting palmar pressure in swing-

through crutch gait. Results indicated that the wrist extension angle was reduced significantly and uniformly during crutch gait, and the peak palmar pressure was redirected from the mid palmar region to the adductor pollicis for six out of ten subjects. However, the wrist still experienced the same loads during crutch gait.

1.6 SOFT PNEUMATIC ACTUATORS

In general, soft pneumatic actuators are characterized by absence of rigid structure, unlike pneumatic cylinder actuators, and have advantages such as high power to weight ratio, can be made with inexpensive materials and manufacturing processes, and are safe for human interaction [38,39].

PneuNets Bending Actuators are a class of soft pneumatic actuators developed by the Whitesides Research Group at Harvard [40] (Figure 1.6a). They are made of a series of channels and chambers inside an elastomer. Inflation in the most compliant regions in the structure create bending or twisting motions. The most popular application of this class of actuator has been in compliant grippers where the actuator bends around the object, conforming to its contour and applying a normal force [39]. In addition, it also has been utilized in a design of soft pneumatic glove for hand rehabilitation, where the same mechanism was used to train hand grip motion [41]. However, the range of force that can be transferred by the bending actuators was relatively small.

Fiber Reinforced Elastomeric Enclosures (FREEs) are another class of soft pneumatic actuators made of elastomer tubes reinforced with a network of fibers [42] (Figure 1.6b). Upon actuation, the expansion of the elastomer tube is reinforced by inextensible fibers. The resultant kinetic and kinematic behavior of FREEs have been analyzed [43-45]. With different fiber configurations, this class of actuators can create a variety of motions including contraction, elongation, twisting, coiling and bending [46]. More complicated motions can even be achieved through parallel combination of different FREEs [47]. A subset of well-known commercialized FREEs is the McKibben muscle, or pneumatic artificial muscle [45]. It is a

class of FREEs that can contract and generate relatively large amounts of tensile force upon actuation. These McKibben muscles have been widely applied in bio-inspired robotics and assistive devices [46].

1.7 HARVESTING ENERGY FROM THE GAIT CYCLE

Researchers have explored methods to harvest pneumatic energy from the human gait cycle. Shiraishi et al. proposed a pneumatic assist device in 1996, using upper body weight to power a pneumatically operated assistive device to assist weakened lower limbs [49]. Durfee et al. described an energy-storing fluid power orthosis combined with electrical stimulation that can help with gait of people with thoracic level spinal cord injury [50]. In addition, Chin et al. successfully developed and tested a self-contained energy harvesting ankle-foot orthosis utilizing a bellow pump embedded in the foam sole [51]. In the stance phase of walking, the bellow pump is compressed and coverts kinetic energy to pneumatic energy, generating an average pressure of 169.0 kPa per step.

1.8 PNEUMATIC ELASTOMERIC ACCUMULATOR

Accumulators are commonly used in fluid systems to reduce the deleterious effect of pressure spikes on other components during operation and to store energy temporarily in the system to be used at a later occasion [52]. While hydraulic accumulators have been well developed, accumulators are not commonly seen in the pneumatic system. Close technologies used to store the pressurized air in the pneumatic system include rigid compressed air tanks and spring-loaded air cylinder. Both suffer from disadvantages such as large size, heavy weight, costly material, and relatively low efficiency in energy storage due to heat loss [52]. To address these issues, pneumatic strain energy accumulators have been developed to enable the use of an accumulator in pneumatic systems [53].

The pneumatic elastomeric accumulator (PEA) is a pneumatic version of the strain energy accumulator (SEA), which is a category of accumulators that utilize the hyperelastic behavior of rubber to

store energy in the form of strain energy in fluid system [54]. These accumulators are compact, lightweight, inexpensive, highly efficient and able to produce a constant output, compared with traditional air storage devices [53]. A PEA consists of an expandable elastomer tube enclosed in a rigid shroud constraining radial and longitudinal expansion (Figure 1.7a). When filling, the air pressure in the tube must achieve a threshold pressure, a.k.a. bubble pressure, at which the tube's radius will explain similar to a balloon. The pressure in the PEA drops immediately with the formation of the bubble and stays at a nearly constant fill pressure as the PEA continues to expand until reaching the maximum volume allowed inside the shroud (Figure 1.7b). The PEA stores energy in the form of strain energy in the stretched elastomer utilizing its hyperelastic behavior and pressure energy of the stored gas inside the tube [53]. A constant discharging pressure is also produced during the exhuasting of the PEA.

Researchers have also investigated capturing the fundamental behavior of SEAs using finite element analysis, experimentally validating SEA behavior, developing new materials and geometries to use for SEAs, and advancing manufacturing processes, primarily in hydraulic applications [52, 54]. Advanced material and manufacturing processes have recently been investigated for PEAs [53]. The current application of PEAs is mainly in exhaust gas recycling. With the use of a PEA and a recycling pneumatic circuit, the efficiency of a portable pneumatic ankle-foot orthosis increased from 25-75% under different modes of operation of this medical assistive device [55].

1.9 THESIS OVERVIEW

Given information and motivation presented above, two studies were conducted to investigate using a pneumatic FREE actuator and PEA accumulator to build a self-contained pneumatic ergonomic crutch system to help long-term Lofstrand crutch users.

Chapter 2 presents the design and biomechanical evaluation of a pneumatically-powered sleeve orthosis for Lofstrand crutches that is attached to the crutch cuff. The orthosis was designed to create an

interface between the crutch cuff and the upper extremity to improve the wrist posture, share loads between the hand and the forearm, redistribute and reduce palmar pressure. We present the detailed design of the pneumatic sleeve orthosis and the protocol for human subject testing of the sleeve orthosis. Analysis and interpretation of the results from human subject testing are included. The overall effects of the sleeve orthosis on swing-through and reciprocal crutch gait are discussed in this chapter.

Chapter 3 focuses on the design and validation of a pair of pneumatic ergonomic crutches (PEC). Each crutch was designed to include the pneumatic sleeve orthosis, an energy harvesting system to collect pressurized air during crutch gait, an energy storage system to accumulate the pressurized air, and a pneumatic circuit control system to charge, exhaust or lock the pneumatic sleeve orthosis. We focus on the modeling of the charging processes and design of the energy harvesting and storage systems. Results from bench-top testing validating the performance of the PEC are presented. In addition, protocols for future human subject testing of the PEC are also included in this chapter.

Chapter 4 summarizes the findings in chapter 2 and chapter 3, reviews the design concept of integrating a pneumatic system into Lofstrand crutch to help with crutch user, and discuss implications of these studies.

1.10 FIGURES

(a) (b) (c) (d) (e)

Figure 1.1. Crutch designs: (a) axillary crutch (Medline Industries, Inc., Northfield, Illinois), (b) Lofstrand crutch (Medline Industries, Inc., Northfield, Illinois), (c) platform crutch (Merya GmbH, Vlotho, Germany), (d) Lofstrand crutch with angle forearm platform (Smart Crutch, Inc., CA), (e) Spring-loaded Lofstrand crutch (Ergobaum forearm crutches, Ergoactives Orthopedic Device Company, Hallandale Beach, FL).

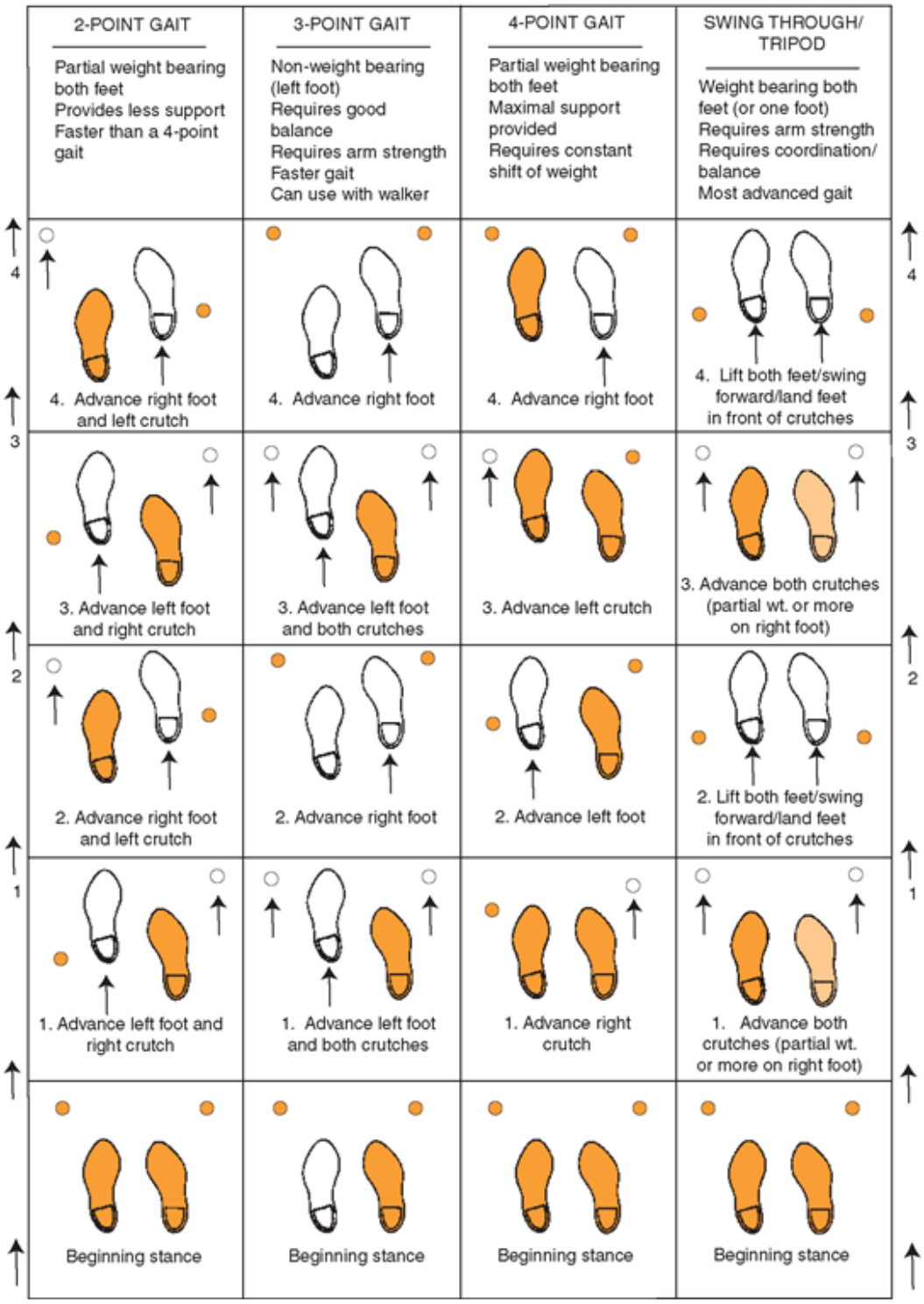

Figure 1.2. Crutch gait patterns [4]

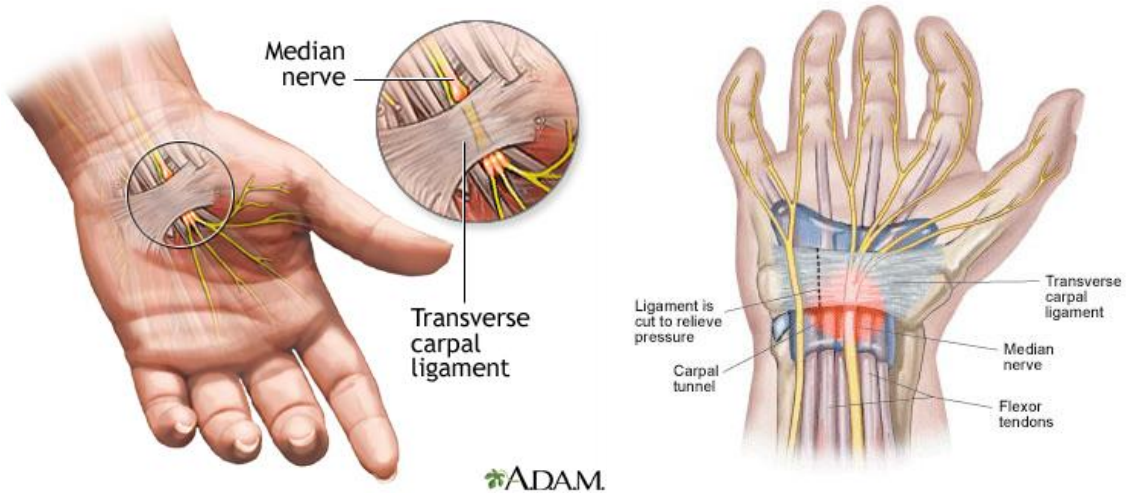

(a) (b)

Figure 1.3. (a) Locations of the carpal tunnel and the median nerve which runs through the carpel tunnel [70], (b) view from another angle [71].

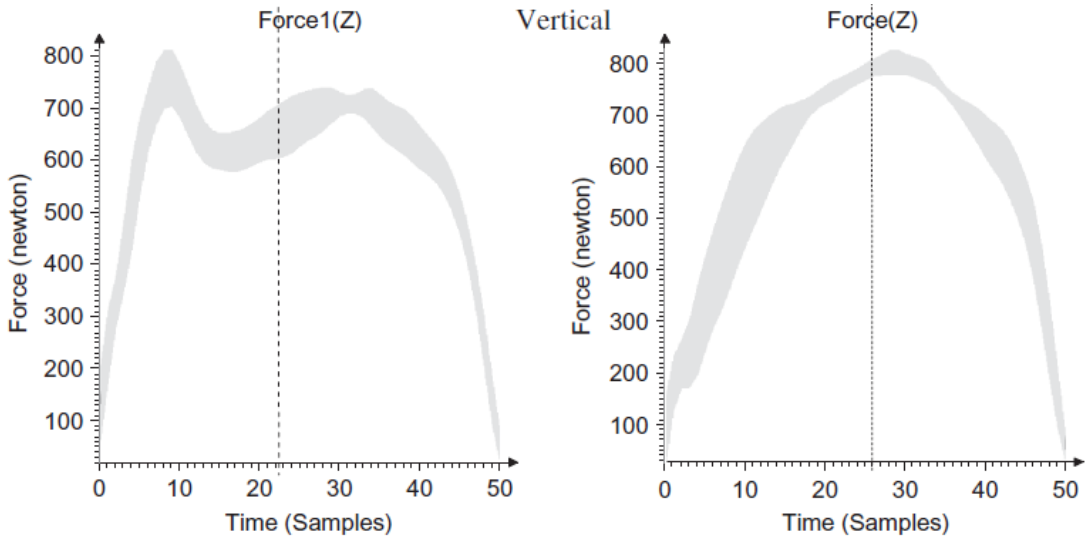

Figure 1.4. Reproduction of Figure 3 from [30]. Vertical ground reaction forces for subject 1 while using traditional Lofstrand crutch (left) and spring-loaded crutch (right). Time was normalized to 50 frames. Shaded areas = ±1 standard deviation. The two vertical dashed lines mark mid-stance time.

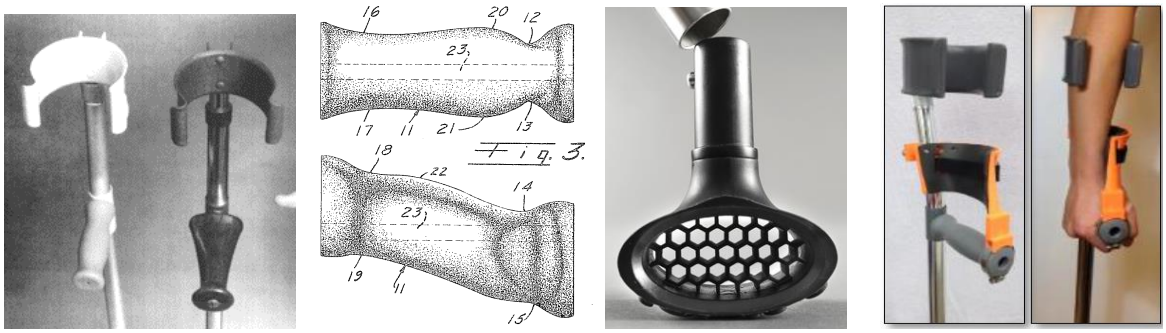

(a) (b) (c) (d)

Figure 1.5. (a) A wide grip on the right compared with standard cylindrical grip on the left [35], (b) Ergonomic crutch handle [36], (c) A compliant crutch tip in the design of M+D crutch (M+D crutch, Mobility Designed, LLC. Kansas City, MO), (d) A wrist orthosis (orange) attached to a Lofstrand crutch [37].

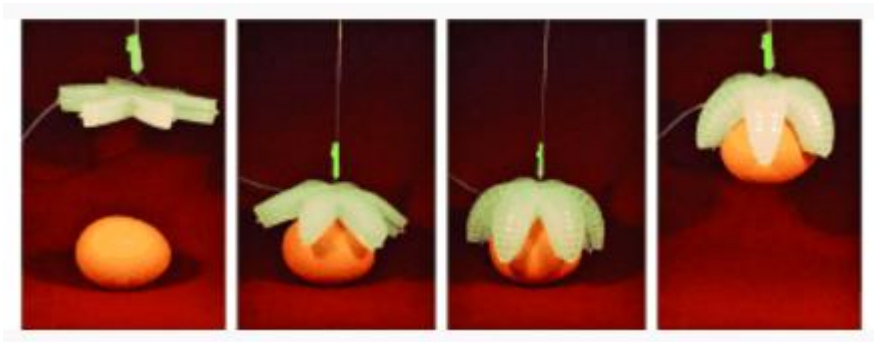

(a)

(b)

Figure 1.6. (a) A demonstration of the PneuNet actuator [39], (b) Schematic of a fiber-reinforced elastomeric enclosure (FREE) with two families of helical fiber at angles α and β [44].

(a)

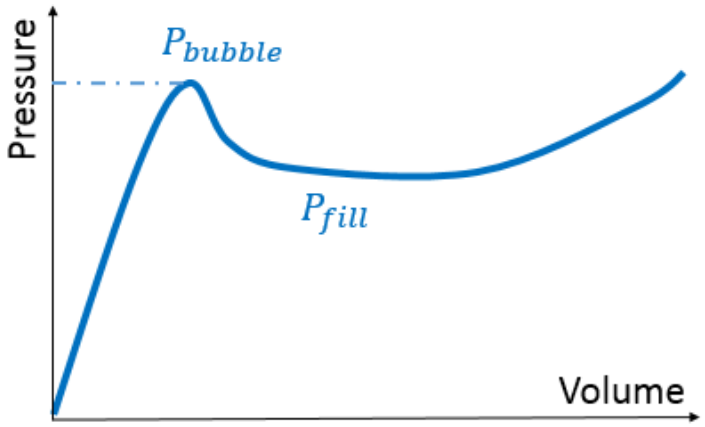

(b)

Figure 1.7. (a) Prototype of PEA in a rigid shroud with a bubbled section, (b) Reproduction of a typical Pressure-Volume relationship of PEA [53]

CHAPTER 2: PNEUMATIC SLEEVE ORTHOSIS FOR LOFSTRAND CRUTCHES

ABSTRACT

Crutch walking, especially when using a double-legged swing-through gait pattern, is associated with repetitive high forces, hyperextension and ulnar deviation of the wrist, and excessive palmar pressure compressing the median nerve. To address these issues, a pneumatic sleeve orthosis was designed for long-term Lofstrand (forearm) crutch users. This sleeve orthosis utilized a soft pneumatic actuator coiled around the forearm and secured to the crutch cuff to share the loads between the hand and forearm. Eleven young healthy adult subjects performed both swing-through and reciprocal crutch gait patterns with and without the orthosis. Wrist kinematics, crutch forces, and palmar pressure were analyzed. Subjects significantly improved wrist posture with orthosis use ($p<0.05$): reductions in peak and mean wrist extension (-6.89%, -6.00%), wrist range of motion (-22.91%), and peak and mean ulnar deviation (-25.69%, -32.02%). The crutch cuff experienced significantly higher forces, as the result of load sharing: increased peak and mean cuff force (both >100%). Peak and mean palmar pressures were also significantly reduced (-8.36%, -10.53%). In addition, a shift of the peak pressure location away from the carpal tunnel region was observed in more than half of the subjects. No significant differences due to orthosis use were identified in reciprocal gait trials; although, similar non-statistically significant trends were observed in the above parameters. These results suggest that Lofstrand crutches modified with a pneumatic sleeve orthosis may be effective at improving wrist posture, reducing wrist and palmar load, and redirecting palmar pressure away from the carpal tunnel region.

2.1 INTRODUCTION

Long term crutch users utilize forearm crutches, also known as Lofstrand crutches, for locomotion commonly using swing-through or reciprocal gait patterns (Figures 2.1, 2.2) [4]. During crutch walking, a single hand and wrist of the crutch user can experience loads up to 45% body weight during swing-through gait and up to 25% body weight during reciprocal gait, along with hyperextension and ulnar deviation of the wrist [9-12]. Such repetitive, large loads and extreme wrist postures may lead to wrist strain, joint pain, and the development of carpal tunnel syndrome (CTS) [14-16, 25, 26]. Studies have also shown that CTS is highly associated with increasing carpal tunnel pressure due to repetitive wrist hyperextension and deviation [19, 22]. High externally applied force on the mid palm region compressing the median nerve can also cause the onset of CTS (Figure 2.3) [20].

Designers and engineers have explored various designs of crutches and attachments to help with Lofstrand crutch users. Spring-loaded Lofstrand crutches have been developed to provide shock absorption and increase the mechanical efficiency when walking with crutches [30, 33]. However, an increased peak ground reaction force was observed [30]. An ergonomic crutch grip has also been designed with extra padding and curvatures to redistribute palmar pressure and guide the hand to a more neutral posture [36]. Nevertheless, no scientific results were found indicating the effectiveness of the ergonomic grip in terms of palmar pressure redistribution and wrist posture improvement.

To address these issues, we previously designed a passive orthosis (Figure 2.4) attached to the crutch handle that was intended to reduce wrist extension and redistribute loads away from the carpal tunnel region on the palm [37]. It was found that providing a wrist support to crutch users significantly improved the wrist posture and redirected the peak pressure away from the carpal tunnel region to the adductor pollicis area. However, all loads still passed through the palm and the wrist. Hence, we aimed to design an orthosis attached to the crutch cuff that was capable of improving the wrist posture, redirecting pressure concentration away from the mid palmar region, and reducing the wrist force by sharing the

loads between the wrist and the forearm. This new orthosis design used an active pneumatic sleeve attached to the crutch cuff that utilized a light-weight yet powerful soft pneumatic actuator to provide a snug constriction force about the forearm. By attaching the orthosis to the crutch cuff and creating a connection between the orthosis and the forearm, we aimed to have the orthosis transfer partial loads from the wrist and hand to the forearm.

The soft pneumatic actuator used in this design is called a Fiber Reinforced Elastomeric Enclosure (FREE) and has several advantages over traditional rigid actuators [44]. A FREE is made of an extensible elastomer tube constrained by families of inextensible fibers coiled around the elastomer tube (Figure 2.5a). Different motion patterns including pure translation (contraction or extension), pure rotation and a screw motion can be generated with different combinations of fiber configurations [44]. The type of FREE actuator used in this study has two families of fibers at equal and opposite angles ($\alpha = -\beta$). Upon actuation (i.e., inflation), the radial expansion of the elastomer tube is reinforced by inextensible filberts, thus contracting and generating a tensile force in the longitudinal direction. Due to the absence of rigid components and the unique actuation mechanism, such actuators have higher power to weight ratio, are compliant and soft, thus able to fit the different contours of the human body, and are safer when interacting with people due to their soft nature [44].

Creating a safe and comfortable interaction between the sleeve orthosis and the forearm is crucial for this design and only a small amount of normal force can be applied to the forearm without causing reduction of blood flow. Studies have shown that a normal pressure of 4.00 kPa (30 mmHg) around the forearm is safe for an extended period of time [56]. Grade four compression sleeves or stockings used to prevent the occurrence of venous disorders usually apply a constant constriction pressure from 4.00 to 5.33 kPa (30 to 40 mmHg) [57]. Intermittent pneumatic compression devices used to improve venous circulation can apply cyclic constriction pressures up to 120 mmHg (16.00 kPa) [58]. Therefore, our design needed to provide a constriction pressure of 30 mmHg or less when the user was not loaded on the crutch.

The constriction pressure could increase temporarily, such as during the crutch stance phase, but return to the lower pressure during crutch swing. Such criteria should ensure a safe interaction between the pneumatic sleeve and the user's forearm.

This paper describes the detailed design and testing of the pneumatic sleeve orthosis used on a Lofstrand crutch. The design components and the mechanism of forearm interaction are explained. Biomechanical testing was also conducted to evaluate the effectiveness of the pneumatic sleeve orthosis on healthy young adults performing swing-through gait and reciprocal gait. We aimed to have light-weight and low profile pneumatic sleeve orthosis apply a constriction pressure no higher than 4.00 kPa when the crutch was not loaded. We hypothesized that the orthosis should improve wrist posture of the crutch user by keeping the wrist at a more neutral position when loaded, i.e., decreasing wrist extension and ulnar deviation angle, and restricting the range of motion of wrist extension. We also hypothesized that the force experienced by the crutch cuff would increase with orthosis use, suggesting load sharing between the cuff and handle. We further hypothesized that the palmar pressure magnitude should decrease, and the peak palmar pressure location should shift away from the carpal tunnel region, as the result of the improved wrist posture.

2.2 METHODS – DESIGN OF THE PNEUMATIC SLEEVE ORTHOSIS

To create a physical interface between the cuff and the forearm, we designed the orthosis to apply a moderate constriction force to the forearm, utilizing a contracting FREE coiled around a pair of hinged splints and cushion pads attached to the crutch cuff (Figure 2.6b). The FREE was clamped to the lateral splint at two points (most distal and proximal) along the length, supported on the medial splint at two intermediate points along the length, and was allowed to freely adjust to any other position along the splints. This specific FREE was made of two families of fibers ($\alpha = -\beta = 30°$) wrapped around a rubber tube with an outer diameter of 9.5 mm, inner diameter of 7.9 mm, and undeformed length of 60 cm. With

the ends of the FREE fixed on the splints, the tensile force generated along its length upon actuation would result in a decrease of the coil diameter and apply a constriction force normal to the forearm (Figure 2.6b) [62]. Such constriction force would generate a static friction force between the upper extremity and the crutch cuff. Thus, the body-weight load going through the upper extremity would be supported by both the handle and the cuff, resulting in a reduced wrist force and a reduced palmar pressure. The constriction force also restricts the forearm from moving in the distal direction, which would have additional benefits of improving wrist posture by restricting movement of the forearm tendons and ligaments and thus restrict wrist extension and deviation. With a more neutral and less extending wrist posture, the peak pressure location was expected to shift away from the carpal tunnel region toward the adductor pollicis area.

The splints and cushions were specifically designed to bear loads along the longitudinal direction of the forearm, conform to the contour of the forearm, and redistribute the constriction pressure over a larger forearm surface area (Figure 2.6c). Each splint was composed of four 3D-printed rigid components connected by hinged joints (Polylactic Acid); thus being able to fit different forearm shapes, while still establishing an interface between the forearm and the cuff for load sharing. The cushion pads covered a majority of the forearm area under the coiled FREE. It was composed of two layers of soft fabric (Nylon) sandwiching a thin 3D-printed sheet (Polylactic Acid) with a thickness of 0.4mm, which was for added stiffness. To allow the user to don and doff the unactuated sleeve orthosis freely, the FREE wrapped around the splints formed a coil with a diameter slightly greater than the size of the forearm. To establish a protocol and produce comparable results among users, a pilot study determined that constraining a length of FREE equal to twice the user's forearm girth plus 9.8 cm would be sufficient for most users. To ensure a safe and comfortable constriction pressure, the pilot study also determined that an actuation pressure of 308.2 kPa (30 psig) of the FREE would produce an overall constriction pressure on the forearm of less than 4.00 kPa when the crutch was not loaded.

2.3 METHODS - HUMAN SUBJECT TESTING

2.3.1 Subjects

Human subject testing was conducted to assess the effect of the pneumatic sleeve orthosis attached to Lofstrand crutches. Eleven able-bodied subjects (5M; 18-32 years old; average height 171.6 ± 7.5 cm; average weight 67.34 ± 9.81 kg) were recruited (Table 2.1). The study was approved by the Institutional Review Boards at the University of Wisconsin – Milwaukee (UWM) and the University of Illinois at Urbana-Champaign (UIUC). The human subject testing was conducted at the Mobility Lab at UWM and informed consent was obtained from all participants.

2.3.2 Testing protocol

Joint kinematics, crutch kinetics, palmar and forearm pressure data, and perceived exertion were collected during the test. Kinematic data were collected at 120 fps using a 15-camera motion capture system (T-series, Vicon Motion Systems, Inc., Oxford, UK) and a 39-marker upper extremity marker model (Figure 2.6a) [60]. In addition to upper extremity markers, heel and toe markers were also placed at the calcaneus and second metatarsal head, respectively, to identify gait events. A pair of custom instrumented Lofstrand crutches were used to collect crutch force data at 960 Hz (Figure 2.7b). Each instrumented crutch was embedded with two 6-axis load cells (MCW-6-500, AMTI Inc., Watertown, MA). The lower load cell measured the overall force applied to the crutch shaft below the crutch handle, while the upper load cell measured forces applied to the crutch neck below the crutch cuff. Markers were also placed on the instrumented crutches at anterior and poster sides of the crutch tip, medial and lateral sides of the crutch shaft, and posterior side of the crutch cuff. Palmar pressure on the dominant side for each subject was measured at 60 Hz by a flexible pressure measuring sensor (Pliance Sensor S2129, Novel GmbH., Munich, Germany). This sensor has 16×16 pressure measurement units with 1 cm × 1 cm unit cells. Before the data collection session, the whole sensor was tightly rolled around the handle of the instrumented crutch on

the subject's dominant side (Figure 2.7c). Several rows and columns of the measurement units were turned off to compensate for overlapping of certain measurement areas, resulting in a 13×12 measurement area (Figure 2.7c). A baseline, unloaded trial was taken after the sensor was wrapped around the handle. Four additional 1 cm diameter low-pressure sensors (Pliance Sensor S2011, Novel GmbH., Munich, Germany) were spaced around the inside of the sleeve on the dominant side to collect the constriction pressure applied to the subject's forearm (Figure 2.7c). After finishing each trial, subjects were also asked to evaluate their rate of perceived exertion (RPE), i.e. "How hard did you feel like your body was working" (Table 2.2) [61].

Prior to data collection, each participant was given 15-30 minutes to acclimate to swing-through and reciprocal gait patterns using a pair of un-instrumented Lofstrand crutches under instructions provided in [4]. The lengths of the un-instrumented crutches were adjusted based on the height of each individual subject, as described in [62]. Body height and weight, length, width, and girth of the upper extremities of each participant were recorded. A harness holding the pressure sensors signal analyzer (Pliance-xf-32 Analyzer, Novel GmbH., Munich, Germany) was put on the participant around the waist (Figure 2.6a).

A palm position identification test was done before each subject's data collection trials. In this test, the researcher applied pressure on the pressure mat that was wrapped around the handle at five points along the contour of the participant's hand (Figure 2.7), such that the subject-specific palmar location could be correlated with the mat location in later analysis.

A pneumatic sleeve orthosis was attached and secured to each cuff of the instrumented crutches in walking trails with orthosis. The splint and the cushion were first installed to the cuff. Subjects were then asked to insert the forearm into the orthosis and place the hand on the crutch handle. The length of the FREE actuator constrained on the sleeve orthosis was adjusted based on the protocol described previously. After the FREE was wrapped around the splint, it was inflated slowly using shop air to 308.2

kPa, while the researcher checked with the subject about the comfort of the forearm. A manual shut-off valve was used to lock the pressurized air in the FREE actuator so that the pressure remained nearly unchanged during all trials of a with-orthosis test condition.

In data collection trials, four test conditions were evaluated: swing-through with orthosis, swing-through without orthosis, reciprocal with orthosis, and reciprocal without orthosis. The order of the test conditions was randomized (Table 2.3). Subjects were asked to perform these tasks over a 6-m walkway at a self-selected speed. At least five trials were collected for each condition. Subjects were given a 1-minute rest between each trial and at least 5 minutes of rest between test conditions.

2.3.3 Data processing and statistical analysis

Five good gait cycles were first identified per test condition for each subject. The quality of each subject's gait performance was examined and gait cycles that exhibited an invalid gait pattern were dropped. In swing-through gait trials, the gait cycles were dropped if the subject was performing a highly asymmetric swing-through gait pattern, in which his/her feet took off and stuck the ground at obviously different times. In reciprocal gait trials, the gait cycles were dropped if the subject exhibited an inconsistent gait pattern, i.e., the subject did not strictly follow heel-strike to heel-strike gait pattern. All data for the entire gait type (swing-through or reciprocal) for a given subject were dropped if it was not possible to identify five valid gait cycles in a specific test condition for this subject. Data from all 11 subjects were included in the analysis of the swing-through gait trials (Table 2.4), while only eight subjects' data were included in the analysis of the reciprocal gait trials due to inconsistent gait patterns of two subjects and missing a crucial wrist marker for one subject (Table 2.5).

All kinematic and kinetic data were calculated across the whole crutch gait cycle and averaged per test condition for each subject. A gait cycle in swing-through gait trails was defined as from a toe strike (0%) to the next toe strike of the dominant foot (100%). In reciprocal gait, it was defined as from a heel strike (0%) to the next heel strike (100%) of the dominant foot. Kinematics, crutch forces and pressure

data from these gait cycles were post-processed using Vicon Nexus (V2.5, Vicon Motion Systems, Inc., Oxford, UK), Novel Pliance (pliance/S, Novel GmbH., Munich, Germany) and MATLAB (R2016a, MathWorks, Inc., Natick, MA) software. Wrist flexion-extension angle and radial-ulnar deviation angle on the dominant side were computed using Vicon Nexus software. Peak and mean wrist extension angle per test condition were reported during the crutch stance phase (from crutch strike to crutch off), while wrist flexion-extension range of motion (ROM) and peak and mean ulnar deviation angles were reported across the whole gait cycle. Crutch cuff and shaft forces, normalized by subject body weight, on the dominant side were calculated, and their peak and mean values were reported during the crutch stance phase. Palmar pressure data from active pressure mat cells were normalized by subject body weight. Peak palmar pressure and mean palmar pressure during crutch stance phase were reported. The peak forearm pressure across the four low-pressure sensors was reported across the whole crutch gait cycles in orthosis trials for both gait types, with the averaged peak forearm pressure calculated in crutch stance phase and crutch swing phase. The average rate of perceived exertion score for the first five trials per test condition for each subject was calculated. Mean and standard deviation RPE scores were reported for each test condition.

For each gait type (swing-through or reciprocal), a multivariate analysis of variance (MANOVA) with a significance value of 0.05 was used to assess the difference in nine parameters between walking with and without the orthosis (SPSS Statistics V23.0, IBM Corp., Armonk, NY). The nine parameters included peak and mean wrist extension angle, wrist flexion-extension ROM, peak and mean ulnar deviation angle, peak and mean normalized crutch cuff force, peak and mean normalized palmar pressure. Univariate ANOVAs (significant level of 0.05) were also examined for each parameter if a significance was identified in the MANOVA test.

Furthermore, to assess the effect of pressure redirection, the palmar pressure distribution was presented in a 13×12 color-coded map and the averaged distance between pressure concentration

location and the carpal tunnel location was estimated per test condition. The results from the palmar location identification test were first analyzed to identify six key palmar location on the 13×12 map for each subject (Figure 2.7a). In data collection trials, the dominant hand position on the crutch handle was calculated along the handle's longitudinal and circumferential direction using the 3rd metacarpal (M3), 5th metacarpal (M5), medial crutch neck, and lateral crutch neck Vicon motion markers when the crutch was not loaded in the selected five gait cycles. The longitudinal and circumferential positions of the dominant hand relative to the handle in the first gait cycle after the identification test was used as the baseline. If the relative longitudinal or circumferential positions of the hand changed from this baseline, the result of the palmar location identification test would then be shifted in the corresponding direction to match the actual hand position in the particular selected gait cycle. A color-coded map was constructed per gait cycle using the peak pressure value in each cell. The cell with the largest pressure value was identified as the pressure concentration point. This map was then overlapped with the adjusted palmar location identification test map and the distance from the location of this pressure concentration cell to Location 1 cell (carpal tunnel) was calculated and averaged over five gait cycles per test condition for each subject (Figure 2.7b).

2.4 RESULTS

A significant difference was observed between swing-through gait trials with and without orthosis conditions from the MANOVA test ($p=0.01$). Follow-up univariate ANOVAs identified significant effects of the pneumatic orthosis use during swing-through gait for all analyzed parameters (Table 2.5, Figure 2.8). Joint kinematic results indicated significant reduction in wrist extension and ulnar deviation motion with orthosis use. Peak and mean wrist extension angles during the crutch stance phase were reduced by 6.89% ($p=0.013$) and 6.00% ($p=0.024$), respectively. Wrist extension ROM was also reduced by 22.91% ($p=0.008$). Moreover, throughout the entire gait cycle, peak ulnar deviation angle was reduced by 25.96% ($p=0.029$)

and the mean ulnar deviation angle was reduced by 32.02% (p=0.024). Kinetic results indicated a significant increase in the crutch cuff force and a significant reduction in palmar pressure with orthosis use during the crutch stance phase. Both peak and mean crutch cuff forces increased significantly by more than 100% (p=0.003 and p=0.001). Up to 15.92% of the body weight was transferred to the forearm and supported by the crutch cuff with the use of orthosis, compared with 5.20% of the body weight transferred to the crutch cuff in without orthosis trials. The peak palmar pressure was decreased by 8.36% (p=0.037), and mean palmar pressure was further reduced by 10.55% (p=0.021).

The MANOVA test for reciprocal gait data found no statistically significant differences in analyzed parameters due to orthosis use (p=0.414). However, non-statistically significant trends similar to swing-through gait use were observed among all parameters (Table 2.7, Figure 2.9). Peak and mean wrist extension, ulnar deviation, palmar pressures and wrist extension ROM were less with orthosis use, while peak and mean crutch cuff forces increased.

The distances between the peak pressure location and the carpal tunnel location increased for the majority of subjects with the use of the orthosis. The averaged distance increased by 0.46 cm and 0.66 cm respectively in swing-through gait trials and reciprocal gait trials (Table 2.8, Figure 2.10). During swing-through gait trials, six out of 11 subjects demonstrated shifting of peak pressure location away from the carpal tunnel location towards the adductor pollicis, while peak pressure location was unchanged for three subjects and moved closer to the carpal tunnel region for the remaining two subjects. During reciprocal gait trials, six out of eight subjects demonstrated such pressure shifting, while two subjects had no change.

Similar levels of maximum forearm pressure were observed in both gait types when the crutch was unloaded (Figure 2.11). In swing-through gait trials, subjects experienced an averaged maximum forearm pressure of 4.07 ± 0.52 kPa during the crutch swing phase and 5.53 ± 0.71 kPa during crutch

stance. In reciprocal trials, subject experienced 3.97 ± 0.12 kPa during the crutch swing phase and 4.12 ± 0.15 kPa during the crutch stance phase.

Borg rate of perceived exertion scores were reduced with orthosis use in both gait patterns (Table 2.9). Subjects gave an averaged RPE score of 11.6 ± 1.9 and 8.5 ± 1.6 with orthosis use and 13.2 ± 2.0 and 9.2 ± 2.4 without orthosis for swing-through and reciprocal gait trials, respectively.

2.5 DISCUSSION

The pneumatic sleeve orthosis was designed to help long-term Lofstrand crutch users to improve wrist posture, reduce wrist force, and redirect palmar pressure. We hypothesized that the pneumatic sleeve orthosis would be effective in terms of keeping the wrist in a more neutral position by reducing wrist extension and ulnar deviation, reducing forces experienced by the wrist through sharing loads between the forearm and the wrist, and reducing loading near the median nerve in the carpal tunnel by reducing peak palmar pressure magnitude and shifting its location away from the carpal tunnel region. In addition, the sleeve orthosis should apply a comfortable constriction pressure around the user's forearm, i.e., ≤ 4.00 kPa when the crutches are not weight-bearing.

We analyzed wrist kinematics, crutch forces, palmar and forearm pressures, and perceived exertion to assess the effectiveness of the pneumatic sleeve orthosis during crutch gait. Two crutch gait patterns were examined. Swing-through gait is a more demanding movement pattern where both legs are lifted and swung forward in advance of the crutches while the upper extremities support the entire body weight. Reciprocal gait requires less effort by the upper extremities, where the lower extremity and the contralateral crutch advance forward alternatively. Several key parameters were selected for statistical analysis. Peak and mean wrist extension angles, wrist flexion-extension ROM, along with peak and mean ulnar deviation angles were used to evaluate wrist posture. Peak and mean cuff forces during crutch stance phase were used to assess the effect of load sharing. Peak and mean palmar pressure during

crutch stance phase were included to assess the effectiveness of reducing palmar pressure. Palmar pressure distribution was analyzed to evaluate the effect of pressure redirection.

Statistical test results found a significant effect of the pneumatic sleeve orthosis when a swing-through gait pattern was used (MANOVA p=0.01). Wrist kinematic data indicated improved wrist posture, such that wrist extension and ulnar deviation angles were significantly decreased when using the orthosis, which resulted in more neutral wrist angles (Table 2.5, Figure 2.7a, 2.7b). Wrist extension ROM during the whole crutch gait cycle was reduced with orthosis use, denoting more restricted flexion-extension of the wrist (Figure 2.7a). Crutch kinetics data demonstrated load sharing between the wrist and forearm as crutch cuff force increased significantly with orthosis use, while the force in the shaft remained the same (Table 2.5, Figure 2.7c, 2.7d). In addition, palmar pressure data indicated a reduced palmar pressure as the peak and mean palmar pressures were reduced significantly with the use of orthosis (Table 2.5, Figure 2.7e, 2.7f). A shift of palmar pressure concentration location, away from carpal tunnel region and toward adductor pollicis, was observed in six out of 11 subjects.

Non-statistically significant trends were observed during reciprocal gait trials (MANOVA p=0.4, Table 2.7). The peak, mean and ROM of wrist extension angles, ulnar deviation angles, and palmar pressures were also reduced, while peak and mean crutch cuff forces were increased (Table 2.7). Moreover, a shift of palmar pressure concentration location, away from carpal tunnel region and toward adductor pollicis, was still observed in the majority of subjects with the use of the orthosis (Table 2.8).

The non-significant results in reciprocal gait could be explained by that the nature of reciprocal gait and the number of samples used in the analysis. Reciprocal gait is less physiologically demanding than swing-through gait due to the existence of double support when the contralateral foot and ipsilateral crutch are in contact with the ground during the ipsilateral leg swing phase. In this case, only a small portion of the body weight is supported by the crutch. In addition, the wrist extension and extension ROM are less extreme compared with those in swing-through crutch gait [9-12]. It should also be noted that

due to inconsistent gait style and absence of one crucial marker, only eight of 11 subjects' data were analyzed in reciprocal gait trials. A reduced sample size might have caused reduced statistical power.

The constriction pressure applied to user's forearm can be further optimized. A constriction pressure ≤ 4.00 kPa is considered safe to be applied to the human skin for an extended period of time, without causing reduction in blood flow and discomfort [65]. The average peak constriction pressure during the crutch swing phase in swing-through gait trials was 4.07 kPa, while the average pressure during reciprocal trials was 3.97 kPa. It should be noted that the actuation pressure of the pneumatic sleeve orthosis was set to 308.2 kPa with the effective length of the FREE (i.e., length of the FREE constrained on the sleeve orthosis) adjusted for each subject to ensure a similar level of constriction force in this study. The actuation pressure and the effective length of the FREE can be further customized for each individual subject to achieve the best effectiveness of the pneumatic sleeve orthosis and a user-selected constriction pressure during the interaction of the device and the forearm.

Perceived exertion scores indicated less effort in completing the task with the use of the orthosis in both gait types (Table 2.9). It was also noticed that the RPE scores were generally smaller in reciprocal trials, which was expected since subjects utilized the lower extremities to support partial body weight due to the nature of the reciprocal gait pattern, resulting in a reduced perceived exertion.

There are some limitations of this study such as using able-bodied subjects and low sample number. The tests were conducted on healthy able-bodied subjects performing crutch gaits, rather than long-term crutch users. Even though all subjects received crutch gait training before starting data collection, their gait pattern could still be different from those of long-term crutch users. Previous researchers had found a significant increase in the crutch stance time and decrease in hip movement for long-term crutch users compared with healthy subjects, due to diminished strength in the lower extremities among crutch users [13]. In addition, the sample size is relatively small for this study. Only data from 11 subjects were collected in swing-through gait trials while data from a fewer number of

subjects were selected in reciprocal gait trials. Lower sample size might have reduced the statistical power as well as the accuracy of the statistical analysis results.

2.6 CONCLUSIONS

We have designed a pneumatic sleeve orthosis utilizing a soft pneumatic actuator and demonstrated its effectiveness of improving wrist posture, sharing wrist force, and reducing and redirecting palmar pressure while safely interacting with users of Lofstrand crutches. The effects are most dramatic in the more biomechanically taxing swing-through crutch gait. Peak and mean wrist extension angles, wrist extension ROM, and peak and mean ulnar deviation angles were significantly reduced, peak and mean crutch forces were significantly increased and peak and mean palmar pressures were significantly decreased. Even though no statistically significant differences were identified in reciprocal gait trials, similar trends were observed from these results. In addition, a shift of pressure concentration away from carpal tunnel region was observed with the use of the orthosis. The distance between the pressure concentration location and carpal tunnel region increased for the majority of subjects in both gait types. Furthermore, the pneumatic sleeve orthosis applied a comfortable constriction pressure to the forearm when the crutch was not loaded and could still be optimized to maximize its effectiveness for individual subject. The reduced RPE scores in trials with orthosis also indicated a reduced perceived exertion during crutch gait using Lofstrand crutches modified with the pneumatic sleeve orthosis.

The statistically significant findings in swing-through crutch gait trials and non-statistically significant trends in reciprocal trials, along with results from palmar pressure distribution, suggest potential clinical impact for crutch users. The improved wrist posture and restricted hyperextension could reduce median nerve pressure and development of carpal tunnel syndrome. The significant increase in the crutch cuff force indicated increased load sharing between the wrist and the forearm. Since the total amount of force going through the crutch shaft was similar with and without the use of orthosis, the increased load in the cuff with the use of orthosis indicated decreased load in the handle in this condition.

In this case, the force experienced by the wrist through the crutch handle was reduced with the use of the orthosis, suggesting a lowered risk of wrist joint injuries. Moreover, the reduced peak pressure magnitude and redirected peak pressure location also indicated reduced carpal tunnel pressure due to reduced externally applied pressure. In this case, this promising pneumatic sleeve orthosis may assist long-term crutch users by producing a more neutral wrist posture and lowering wrist and palm force to alleviate and prevent the development of wrist pain and carpal tunnel syndrome.

2.7 FIGURES & TABLES

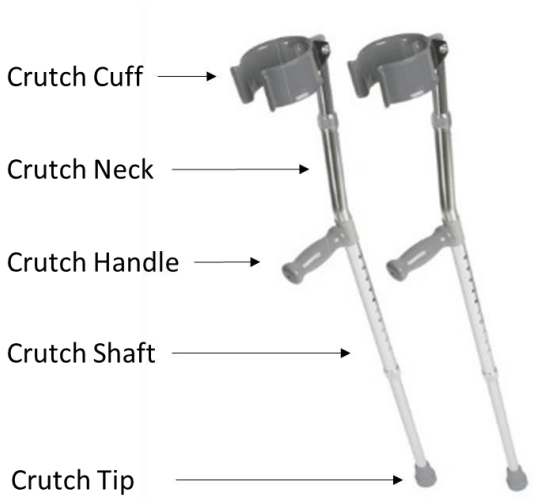

Figure 2.1. Key components of a pair of standard Lofstrand crutches (Medline Industries, Inc., Northfield, Illinois)

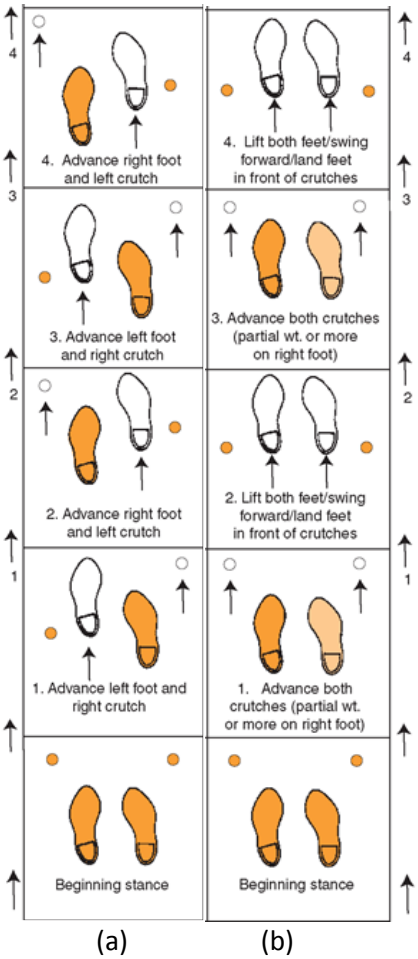

Figure 2.2. Crutch gait pattern: (a) reciprocal gait, and (b) swing-through gait [4]

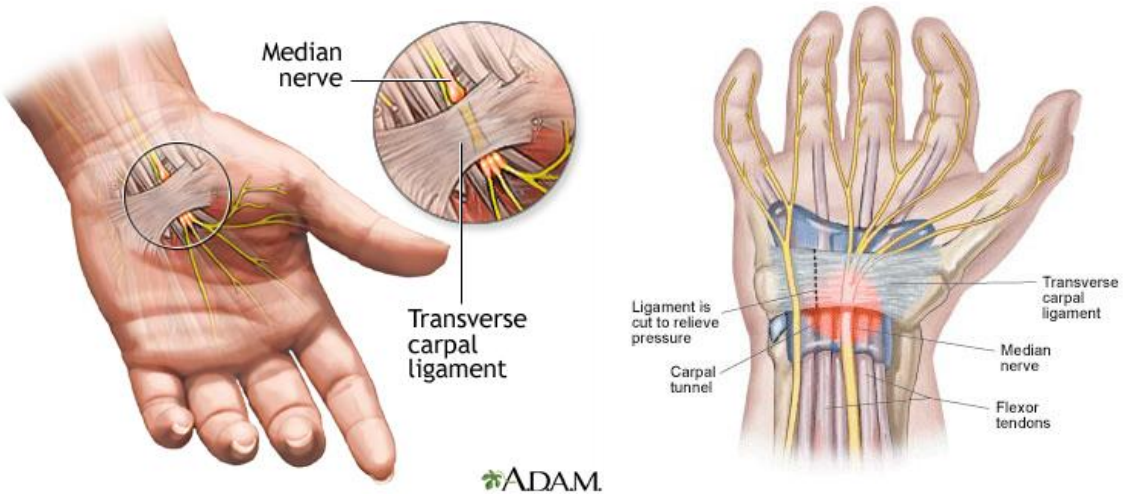

(b) (b)

Figure 2.3. (a) Locations of the carpal tunnel and the median nerve which runs through the carpel tunnel [70], (b) view from another angle [71].

Figure 2.4. Wrist Orthosis (orange) attached to a Lofstrand crutch [37].

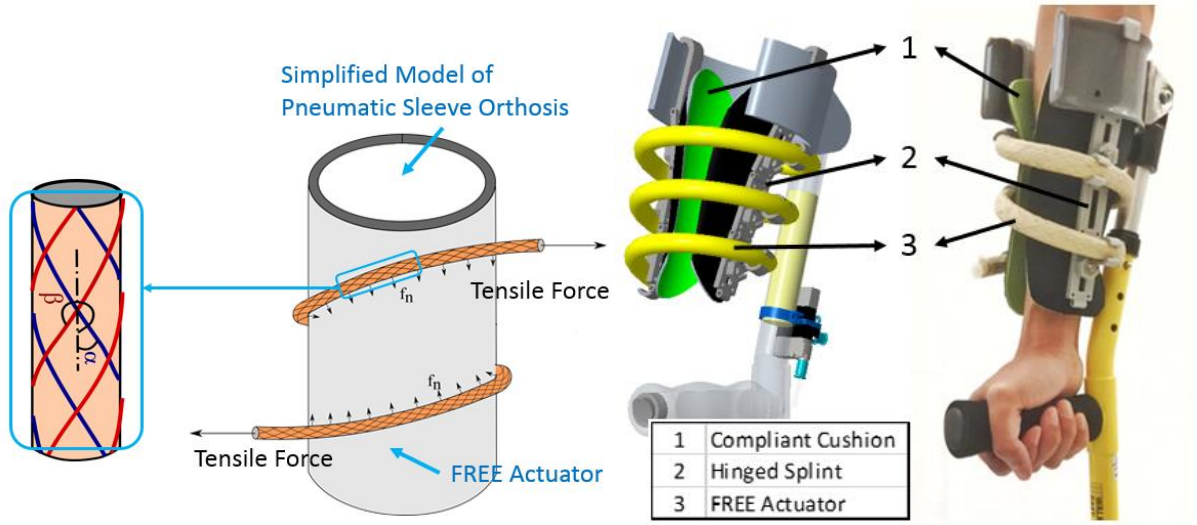

(a) (b) (c)

Figure 2.5. (a) A fiber-reinforced elastomeric enclosure (FREE) with two families of helical fiber at angles α and β (blue, red) [44], (b) Illustration of FREE Actuator and generation of constriction force in coiled configuration [63] [62], (c) CAD and prototype of the Pneumatic Sleeve Orthosis

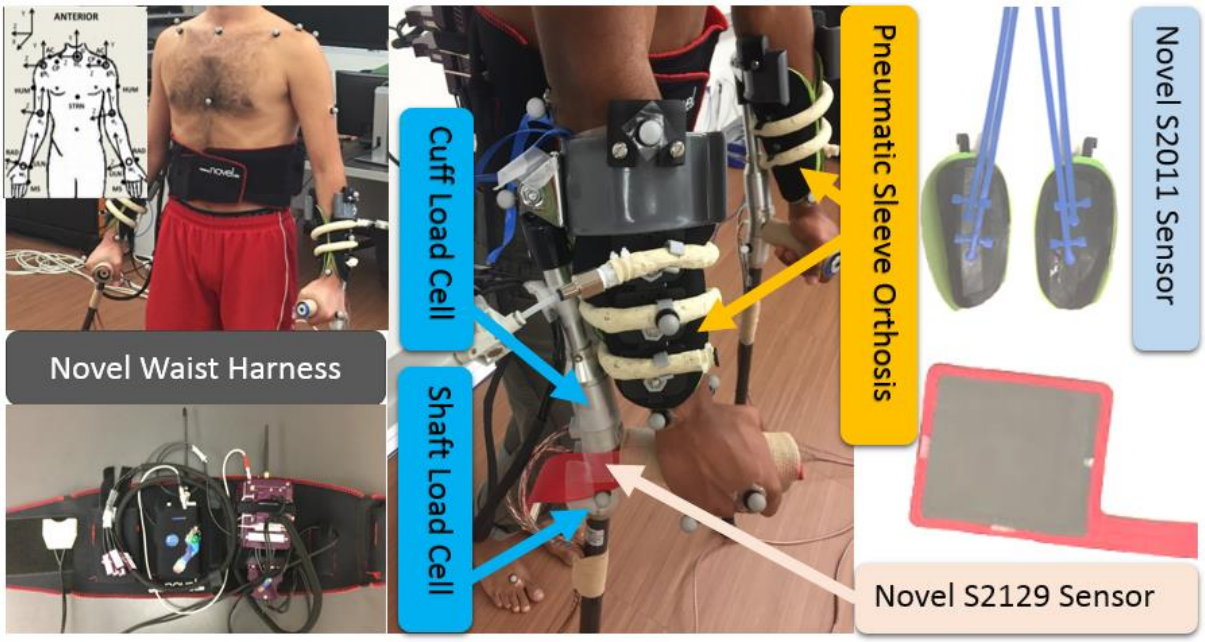

(a) (b) (c)

Figure 2.6. Subject during data collection with all sensors (a) Subject with markers & waist harness, (b) Instrumented crutches with embedded load cells, (c) Pressure sensor S2129 wrapped around the crutch handle and four S2011 sensor attached to the inside of the sleeve orthosis.

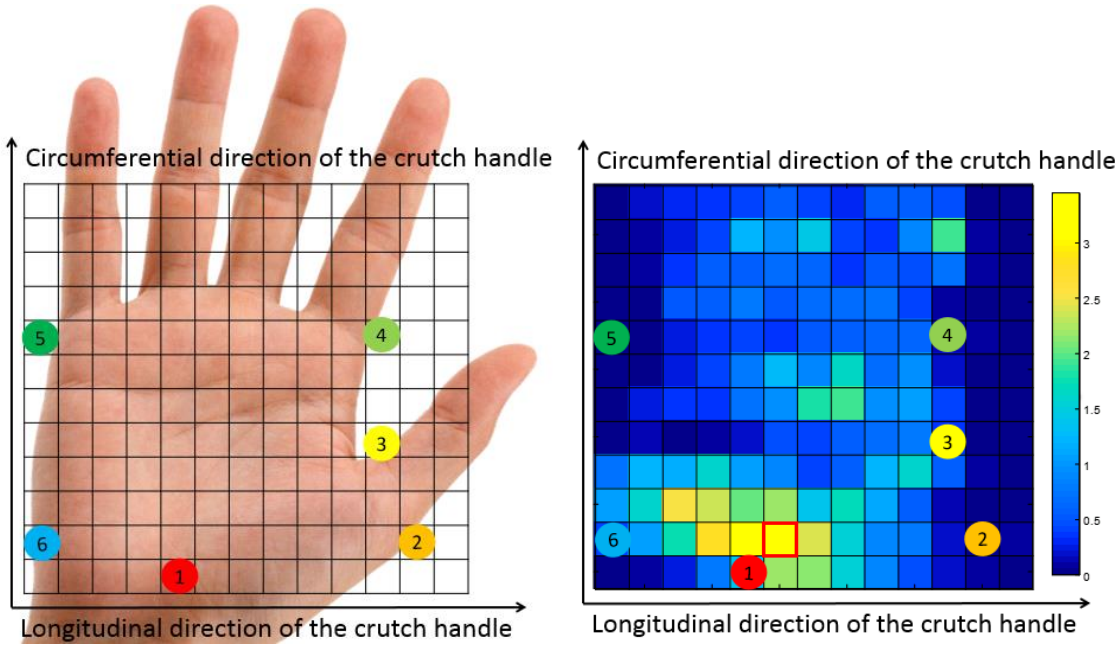

(a) (b)

Figure 2.7. Illustrations for palm location identification test and exemplary results, location 1 is the carpal tunnel, (b) overlapping of the pressure distribution map and results from (a), red square is the pressure concentration location.

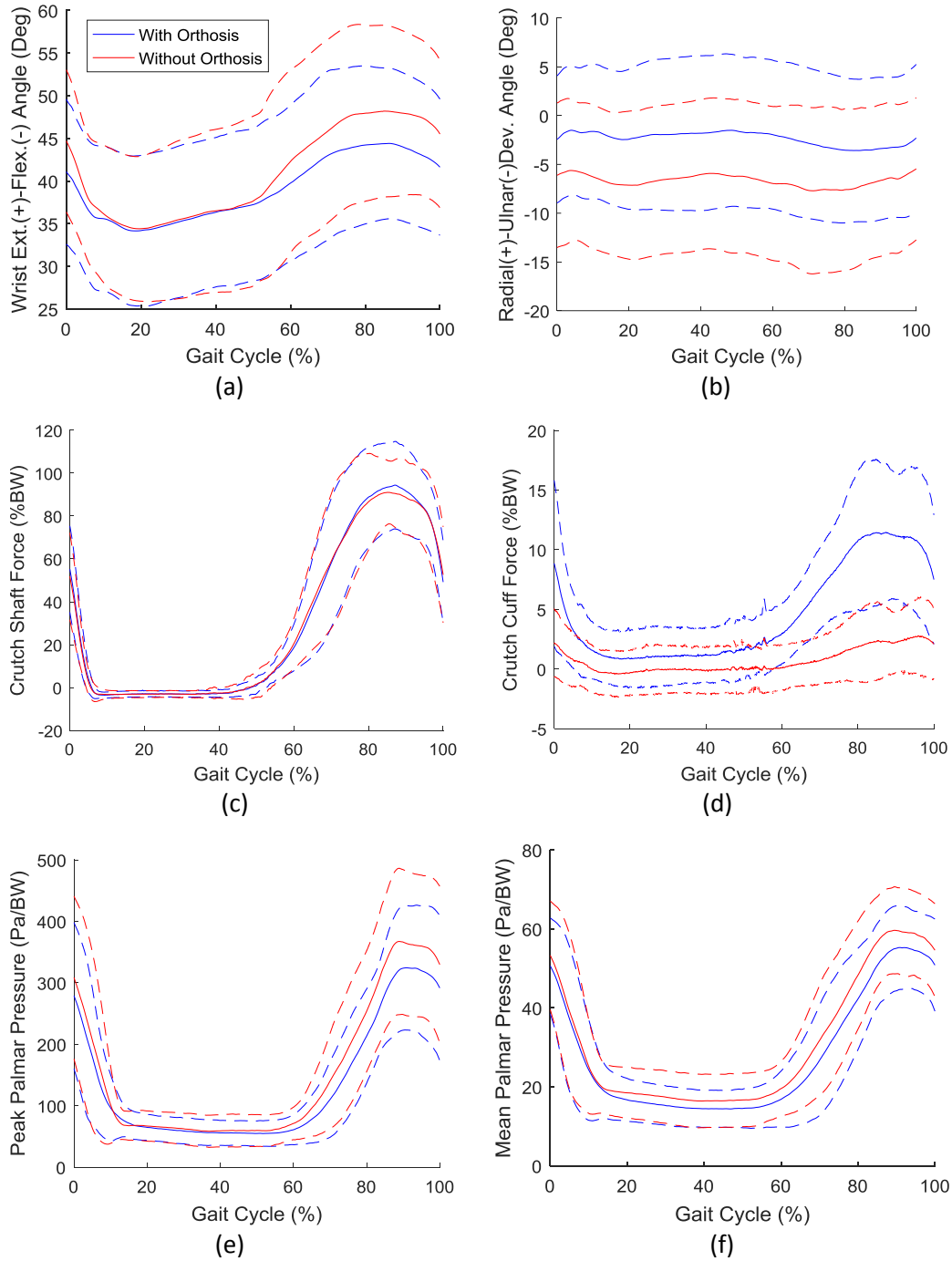

Figure 2.8. Average (solid) and one standard deviation (dashed) kinematics and kinetics during swing-through gait with and without use of the pneumatic sleeve orthosis. Ensemble averages across 11 subjects. (a) Wrist extension angle, (b) Radial-ulnar deviation angle, (c) Crutch shaft force, (d) Crutch cuff force, (e) Peak palmar pressure, (f) Mean palmar pressure.

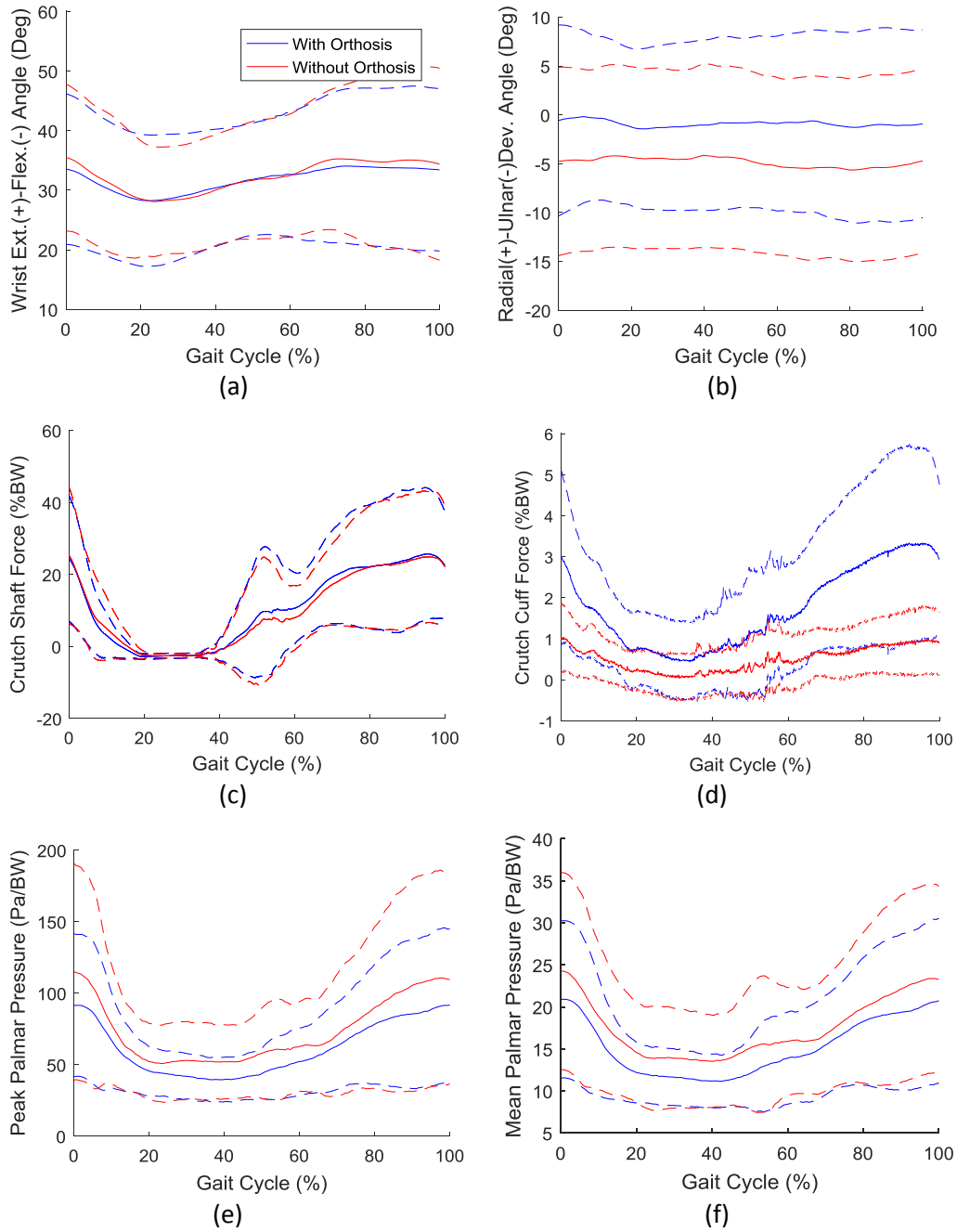

Figure 2.9. Average (solid) and one standard deviation (dashed) kinematics and kinetics during reciprocal gait with and without use of the pneumatic sleeve orthosis. Ensemble averages across 8 subjects. (a) Wrist extension angle, (b) Radial-ulnar deviation angle, (c) Crutch shaft force, (d) Crutch cuff force, (e) Peak palmar pressure, (f) Mean palmar pressure.

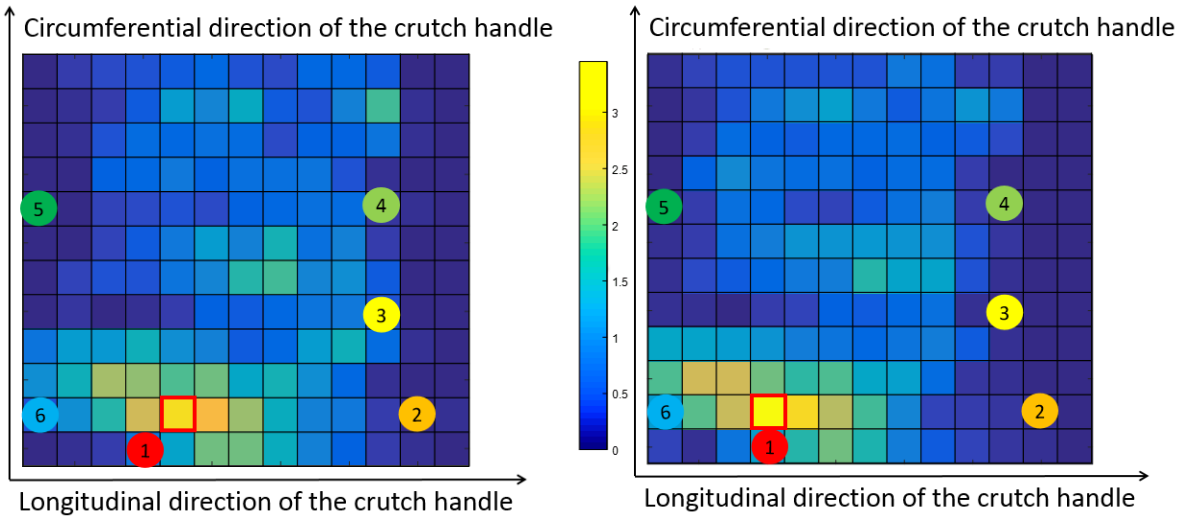

Figure 2.10. Visualization of peak palmar pressure distribution of a representative subject: pressure distribution during swing-through gait trials with (a) and without (b) orthosis use; we can clearly see that the pressure concentration point shifted to the right from (b) to (a), which is the direction away from carpal tunnel, and the magnitude of the peak pressure dropped.

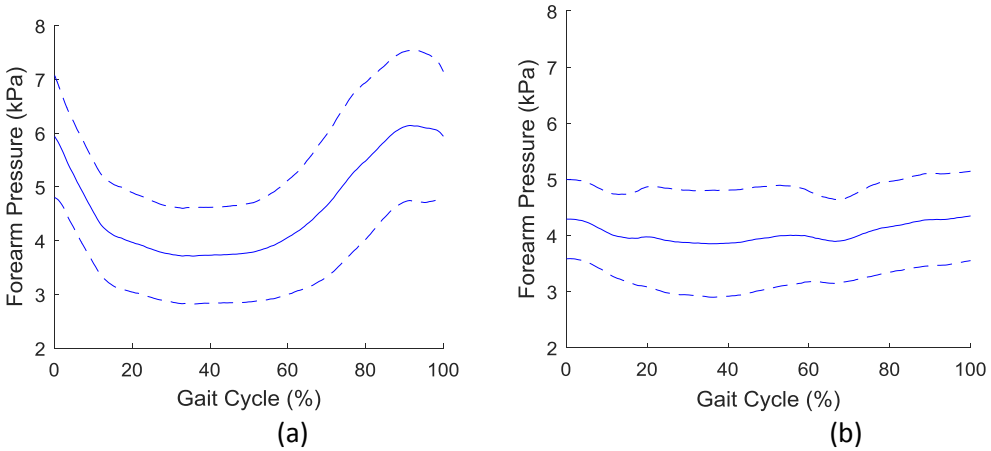

Figure 2.11. Maximum forearm pressure all for subjects in (a) swing-through gait trials (b) reciprocal gait trials, averaged over 11 subjects

Table 2.1. *Subject Demographics*

Subject ID	Age	Sex	Handedness	Height(m)	Weight(kg)
1	24	M	Right	1.83	75.74
2	18	M	Right	1.71	61.16
3	21	F	Right	1.68	61.16
4	21	M	Right	1.64	61.61
5	21	M	Left	1.73	81.99
6	23	F	Right	1.69	65.23
7	32	M	Right	1.85	80.82
8	23	F	Right	1.68	60.34
9	22	M	Right	1.66	60.16
10	24	F	Right	1.79	78.19
11	24	F	Right	1.64	54.36
Average	23 ± 3.5	5M/6F	10R/1L	1.72 ± 0.75	67.34 ± 9.81

Table 2.2. *Borg's Perceived Exertion Scale [10]*

Rating	Perceived Exertion
6	
7	Very, very light
8	
9	Very light
10	
11	Fairly light
12	
13	Somewhat hard
14	
15	Hard
16	
17	Very hard
18	
19	Very, very hard
20	

Table 2.3. *Testing Order for Each Subject*
(ST: swing-through gait; RP: reciprocal gait; 1: with orthosis; 0: without orthosis)

Subject ID	ST1	RP1	ST0	RP0
01	1	2	3	4
02	4	2	3	1
03	3	1	2	4
04	1	2	4	3
05	2	1	4	3
06	3	4	2	1
07	1	2	3	4
08	2	1	4	3
09	1	2	4	3
10	4	3	1	2
11	3	4	1	2

Table 2.4. *Data Quality for Subjects Performing Swing-Through Gait*

Subject ID	Gait Behavior	Wrist Kinematics	Crutch Forces	Pressures
01	Symmetric	✓	✓	✓
02	Symmetric	✓	✓	✓
03	Symmetric	✓	✓	✓
04	Symmetric	✓	✓	✓
05	Symmetric	✓	✓	✓
06	Symmetric	✓	✓	✓
07	Symmetric	✓	✓	✓
08	Symmetric	✓	✓	✓
09	Symmetric	✓	✓	✓
10	Symmetric	✓	✓	✓
11	Symmetric	✓	✓	✓

Table 2.5. *Results for Swing-Through Gait Trials: Mean (Standard Deviation), Percentage Difference from Without Orthosis Conditions, and Univariate ANOVA p-values (MANOVA p = 0.01)*

Measures	With	Without	Difference	P-value
Peak Wrist Ext. Angle (deg)*	46.38 (9.10)	49.81 (9.52)	-6.89%	0.013
ROM of Wrist Ext. Angle (deg)*	12.55 (5.34)	16.28 (5.00)	-22.91%	0.008
Mean Wrist Ext. Angle (deg)*	42.65 (8.62)	45.37 (9.44)	-6.00%	0.024
Peak Wrist Dev. Angle (deg)*	8.70 (3.53)	11.75 (4.62)	-25.96%	**0.029**
Mean Wrist Dev. Angle (deg)*	6.43 (4.04)	9.46 (4.52)	-32.02%	**0.024**
Peak Cuff Force (%BW)*	15.92 (12.55)	5.20 (4.18)	>100%	**0.003**
Mean Cuff Force (%BW)*	4.49 (2.76)	0.10 (0.17)	>100%	**0.001**
Peak Palmar Pressure (Pa/BW)*	358.16 (125.51)	390.82 (115.31)	-8.36%	**0.037**
Mean Palmar Pressure (Pa/BW)*	34.69 (7.14)	38.78 (8.16)	-10.53%	**0.021**

(: p value < 0.05)*

Table 2.6. *Data Quality for Subjects Performing Reciprocal Gait*

Subject ID	Gait Behavior	Wrist Kinematics	Crutch Forces	Pressures
01	Consistent heel strike	✓	✓	✓
02	Consistent heel strike	✓	✓	✓
03	Consistent heel strike	✓	✓	✓
04	Inconsistent striking	×	×	×
05	Consistent heel strike	×	✓	✓
06	Consistent heel strike	✓	✓	✓
07	Consistent heel strike	✓	✓	✓
08	Consistent heel strike	✓	✓	✓
09	Inconsistent striking	×	×	×
10	Consistent heel strike	✓	✓	✓
11	Consistent heel strike	✓	✓	✓

Table 2.7. *Results for Reciprocal Crutch Gait Trials: Mean (Standard Deviation), Percentage Difference from Without Orthosis Conditions (Univariate ANOVA p-values not applicable since MANOVA p = 0.4)*

Measures	With	Without	Difference
Peak Wrist Ext. Angle (deg)	36.47 (12.27)	38.51 (11.63)	-5.30%
ROM of Wrist Ext. Angle (deg)	9.89 (4.43)	13.06 (5.54)	-24.27%
Mean Wrist Ext. Angle (deg)	33.33 (12.11)	34.14 (12.31)	-2.37%
Peak Wrist Dev. Angle (deg)	9.89 (4.17)	11.68 (4.39)	-15.32%
Mean Wrist Dev. Angle (deg)	7.65(4.75)	9.04 (5.12)	-15.37%
Peak Cuff Force (%BW)	5.71 (2.14)	3.37 (1.12)	69.70%
Mean Cuff Force (%BW)	2.55 (1.53)	0.82 (0.71)	>100%
Peak Palmar Pressure (Pa/BW)	107.14 (57.14)	127.55 (79.59)	-16.00%
Mean Palmar Pressure (Pa/BW)	16.22 (6.12)	18.27 (7.14)	11.11%

Table 2.8. *Palmar Distance between Pressure Concentration Location and Carpal Tuneel Location for Each Subject During Swing-through or Reciprocal Gait Trials*
(: the lower palmar distance between the pressure concentration location and the carpal tunnel location)*

	Swing-through		Reciprocal	
Subject ID	with orthosis	without orthosis	with orthosis	without orthosis
01	1.41 cm	1.41 cm	2.82 cm	1.41 cm*
02	1.41 cm	1.00 cm*	0.00 cm	0.00 cm
03	2.00 cm	1.00 cm*	4.00 cm	3.00 cm*
04	1.00 cm	0.00 cm*	-	-
05	1.00 cm	0.00 cm*	-	-
06	1.72 cm*	1.80 cm	1.72 cm	1.00 cm*
07	2.00 cm	2.00 cm	2.23 cm	2.00 cm*
08	2.23 cm	2.23 cm	3.16 cm	3.16 cm
09	2.00 cm	2.00 cm	-	-
10	3.16 cm	1.41 cm*	3.60 cm	1.72 cm*
11	1.00 cm	1.00 cm	1.12 cm	1.00 cm*
Average	1.72 ± 0.66 cm	1.26 ± 0.76 cm	2.33 ± 1.34 cm	1.66 ± 1.06 cm

Figure 2.9. *Borg's Perceived Exertion Scores for Each Subject*

	Swing-through		Reciprocal	
Subject ID	**with**	**without**	**with**	**without**
01	10.8	12.8	7.5	8.0
02	12.0	12.7	8.0	8.0
03	13.1	14.0	12.0	11.3
04	11.0	14.8	9.2	14.2
05	9.0	9.2	7.0	7.0
06	14.0	16.3	8.0	10.8
07	11.8	12.7	6.7	6.3
08	14.5	15.0	10.0	11.0
09	9.2	12.2	7.7	7.0
10	12.7	14.8	9.8	9.0
11	9.3	11.0	7.3	8.2
Average	11.6 ± 1.9	13.2 ± 2.0	8.5 ± 1.6	9.2 ± 2.4

CHAPTER 3: DESIGN AND EVALUATION OF PNEUMATIC ERGONOMIC CRUTCHES

ABSTRACT

Repetitive high impulse forces, hyperextension and ulnar deviation of the wrist, and excessive palmar pressure compressing the median nerve experienced by crutch users during crutch gait have been reported to cause joint pain, discomfort and other injuries in the wrist and the hand. To address these issues, we developed a pair of pneumatic ergonomic crutches (PEC). A compressive pneumatic sleeve orthosis was attached to the crutch cuff to improve wrist posture, share load between the wrist and the forearm, and redistribute palmar pressure. We exploit the energetics of walking by integrating a spring-loaded piston pump into the crutch tip to harvest pneumatic energy and provide shock absorption. A pneumatic elastomeric accumulator (PEA) was inserted into the crutch shaft to store the collected pneumatic energy from the piston pump and to use it in the subsequent pressurization of the sleeve orthosis. Analytical expressions were derived to describe the processes of charging the accumulator with the piston pump and charging the sleeve orthosis with the accumulator. Using these expressions, we optimized the bore diameter of the piston shaft, the stroke length of the piston pump, and specifications of the pneumatic elastomeric accumulator to minimize the number of gait cycles used to fully charge the accumulator. Bench-top testing was conducted on the PEC and demonstrated the ability of charging the pneumatic sleeve orthosis using air stored in the PEA after ~38 gait cycles. Protocols for future human subject testing to evaluate the system performance of the PEC are also presented.

3.1 INTRODUCTION

Long term crutch users utilize Lofstrand crutches, or forearm crutches, for ambulation commonly using swing-through or reciprocal gait patterns (Figure 3.1a, 2) [4]. When users load the crutch against the ground, the ground reaction forces (GRFs) at the tip of the crutch are transmitted to the wrist, elbow and shoulder joints through the crutch handle [9]. The palm and wrist of one side of the body can experience loads up to 45% body weight during swing-through gait and up to 25% body weight during reciprocal gait, along with repetitive hyperextension and prolonged ulnar deviation of the wrist [9-12]. During crutch strike, a rapidly increasing impulse force is also transmitted to the hand and wrist [9]. Such combination of conditions has been reported to cause joint discomfort, joint pain and may lead to carpal tunnel syndrome and other serious conditions in long-term crutch users [14, 15, 26-28].

To help with long-term crutch users, people have modified designs of Lofstrand crutches and developed various accessories. Spring-loaded Lofstrand crutches have been developed to provide shock absorption during crutch gait (Figure 3.1b) [30]. The rate of the resultant GRF rise and the magnitude of the resultant GRF at 50, 100, 200 ms of the crutch gait cycle were reduced during spring-loaded crutch-assisted gait (Figure 3.3) [30]. However, a slight increase in the resultant GRF was also observed. An ergonomic crutch handle was developed to redistribute palmar pressure; however, no scientific evaluation was found [36]. In addition, a passive wrist orthosis has also been designed to improve wrist posture and redistribute palmar pressure (Figure 3.4) [37]. Results indicated a significantly improved wrist posture and a shift of pressure concentration from the carpal tunnel region to the adductor pollicis. Nevertheless, all loads still went through the wrist with that design.

To address these issues, we proposed the concept of the pneumatic ergonomic crutches (PEC) (Figure 3.5a). These crutches were developed to help crutch users improve wrist posture, reduce and redirect loads in the palm and wrist, and better absorb shock during crutch gait. The system includes a pneumatic sleeve orthosis attached to the crutch cuff, a pneumatic energy harvesting piston pump in the

crutch tip, a pneumatic elastomeric accumulator enclosed in the crutch shaft to store the harvested air, and a pneumatic circuit control system accessible from the crutch handle. The sleeve is pressurized prior to beginning a walk and depressurized when the crutches are removed, such as when seated for extended periods.

A pneumatic sleeve orthosis was attached to the crutch cuff and created a constriction pressure around the forearm (Figure 3.4). The sleeve orthosis was composed of a soft pneumatic Fiber Reinforced Elastomeric Enclosure (FREE) actuator wrapped around two hinged splints attached to the crutch cuff. Details of the design of the sleeve orthosis were presented in Chapter 2. Due to the support provided by the sleeve orthosis, this modified crutch was found to significantly improve wrist posture by reducing wrist extension and ulnar deviation angles, share the load between the wrist and the forearm, and redirect palmar pressure away from the more potentially harmful carpal tunnel location. However, this design required an external pneumatic energy source (e.g., dedicated shop air line) to inflate the FREE actuator to the desired inflation pressure of 308.2 kPa (30 psig). A self-contained crutch system was desired that include an integrated pneumatic energy source.

To create this self-contained crutch system that worked with the pneumatic sleeve orthosis, we proposed a pneumatic energy harvesting and storage system and the pneumatic circuit control system. When using the PEC, the user first dons the crutch cuff with sleeve and uses the pressurized air stored in the pneumatic elastomeric accumulator (PEA) from the previous walk to pressurize the sleeve orthosis. The piston pump harvests pneumatic energy during crutch gait and stores the collected pressurized air into the PEA. This stored air is then used in the subsequent pressurization of the sleeve orthosis. In this case, the system does not need any external energy source such as a portable air compressor or fixed-volume air canister.

We chose to harvest pneumatic energy from crutch gait by integrating a spring-loaded piston pump into the crutch tip (Figure 3.5b). We aimed to design the piston pump with a comfortable stroke

length and to fully charge the energy storage system within a minimal number of gait cycles. The spring and compressible air were expected to also provide shock absorption by partially absorbing impact energy during the crutch strike.

We chose to use a pneumatic elastic accumulator to store the collected pressurized air from the energy harvesting piston pump (Figure 3.6a). Compared with traditional fixed-volume accumulators, the pneumatic elastomeric accumulator has advantages including lighter weight, higher energy density ratio, and lower cost [53]. It is composed of an elastomer tube enclosed inside a rigid shroud. The PEA exhibits a hyperplastic property and inflates rapidly to fill the space inside the shroud, which stores strain energy in the rubber material [53]. When filling, the air pressure in the tube must achieve a threshold pressure, a.k.a. bubble pressure, at which the tube's radius will explain similar to a balloon. The pressure in the PEA drops immediately with the formation of the bubble and stays at a nearly constant fill pressure as the PEA continues to expand until reaching the maximum volume allowed inside the shroud (Figure 3.6b).

This paper focuses on the design and evaluation of a pair of pneumatic ergonomic crutches. Analytical expressions describing the charging processes and physical constraints in the PEC system were derived. Design parameters of the energy harvesting system and the energy storage system were determined using these expressions. In addition, we present a bench-top test of the PEC to preliminarily demonstrate the performance of energy harvesting, energy storing, and pressurization of the sleeve orthosis. Testing protocol for future human subject testing to evaluate PEC performance and effectiveness of shock absorption onto crutch gait is also presented.

3.2 DESIGN OF THE PNEUMATIC ERGONOMIC CRUTCHES

3.2.1 Design overview

The pneumatic ergonomic crutches (PEC) were designed to contain the pneumatic energy harvesting system, the energy storage system, the sleeve orthosis and the control system (Figure 3.5). We

modified a pair of traditional Lofstrand crutches as the main body (Medline Forearm Crutches, Medline Industries, Inc., Mundelein, IL) and integrated these components into the crutches. The PEC should be able to harvest pneumatic energy during crutch gait, store the energy and use the energy to power the pneumatic sleeve orthosis to a desired actuation pressure effectively and efficiently.

The pneumatic energy harvesting system consisted of the piston pump and pneumatic components (Figure 3.5b). The piston pump was composed of three parts: the main air chamber case, the piston shaft, and the upper case. Piston pump components were machined using Aluminum rod (6061). The main air chamber case was press-fitted into the rubber crutch tip. The piston shaft was attached to the lower end of the metal crutch shaft by screws. An O-ring was inserted into the groove air seal in the piston head. The upper case was attached to the main air chamber case by screws and a sleeve bearing was press-fitted into the upper case, allowing the crutch shaft to slide along the air chamber. To provide an automatic return of the piston once compressed, a conical spring (31.75 mm overall length, 24.77 mm x 12.70 mm outer diameter) was inserted between the piston shaft and the air chamber. Pneumatic circuit components were integrated into the piston pump. A check valve (AKH-04-A-M5, SMC Corp. of America, Noblesville, IN) was screwed to the lower end of the main chamber case which was open to atmosphere inside the rubber crutch tip, while the other check valve was attached to inner tunnel of the piston shaft (Figure 3.5b). When the piston pump is compressed during crutch strike, these check valves will force the air out of the chamber through the piston shaft. When the piston pump leaves the ground, the conical spring and check valves will extend the piston head and crutch tip back to their original positions, in preparation for another compression cycle.

The pneumatic elastomeric accumulator (PEA) was integrated into the crutch shaft as the energy storage system. A PEA usually consists of an elastomer tube enclosed by a rigid shroud, with one end of the tube connected to the pneumatic circuit [ref]. In this design, the crutch shaft (inner diameter of 2.54 cm) was directly used as the shroud to maximize the radial expansion of the PEA. In addition, an in-line

design was adopted for the PEA such that both ends of the tube were connected to the pneumatic circuit. The distal end of the PEA was connected to the piston pump via a check valve, while the proximal end was connected to a pressure relief valve (VFOF, Festo Corp, Hauppauge, NY). The pressure relief valve was set to 515.0 kPa (60 psig) and attached to prevent over-filling of the PEA (Figure 3.5c). During crutch use, after the PEA was fully charged to 515.0 kPa, any air captured by subsequent compressions of the crutch tip and piston pump would be exhausted to atmosphere through the pressure release valve. The PEAs were fabricated using natural latex rubber tubes with inner diameter of 0.32 cm and outer diameter of 0. 80 cm. It should be noted that the elastomer tube should always start inflation at the distal end of the PEA and propagate towards the proximal end, without the occurrence of a second inflation location. If the bubble starts at the proximal end and propagates back towards the distal end, the remaining elastomer tube will be crushed in the limited space and simply stop further expansion [65]. In this case, the elastomer tube was pre-stretched following a protocol to weaken the elastomer near the distal end prior to the assembly of the PEA [65].

The pneumatic sleeve orthosis has been previously designed and was attached to the crutch cuff (see design details in Chapter 2). A second pressure relief valve (VFOF, Festo Corp, Hauppauge, NY) was set to 377.1 kPa (40 psig) and attached to the inlet of the soft pneumatic actuator to prevent it from over-charging (Figure 3.5c).

The PEC required three modes of operation: 1) charge the FREE from the PEA to contract the sleeve at the beginning of a walk, 2) lock the pressurized air in the FREE while letting the piston pump charge the PEA during crutch gait, and 3) discharge the FREE when removing the crutches. In this case, the control circuit (Figure 3.7a) was designed to provide these three modes of operation through combinations of on/off states of two 3/2 way electromechanical solenoid valves (MHP1, Festo Corp., Hauppauge, NY) that were attached to the posterior side of the crutch neck. A 3-state toggle switch (DPDT/on-off-on rocker switch), which was inserted into the crutch handle, was used to control the two

solenoid valves. A battery (3.7V, Lithium polymer battery) and a voltage boost circuit board (Boost Converter, Spark Fun Electronics Inc., Boulder, CO) were inserted into the crutch neck (Figure 3.5c).

3.2.2 Derivation of charging processes and physical constraints

To determine the dimensions for the piston pump (stroke length and bore diameter) and specifications for pneumatic elastomeric accumulator (material, inner diameter, outer diameter, bubble pressure, and fill pressure), we derived analytical expressions that characterized the charging processes of the PEC using these design parameters.

The two charging processes for the PEC were: 1) charge the PEA using the piston pump during crutch gait, and 2) charge the FREE in the sleeve to the desired actuation pressure of 308.2 kPa (30 psig) using air stored in the PEA prior to the beginning of a walk. Assuming the ideal gas law, an isothermal condition, and no losses or leaks in the pneumatic system, the initial and final state of each charging process can be analytically expressed using Boyle's Law (i.e., $V_i P_i = V_f P_f$) as:

1) Using the piston pump to charge the PEA from atmospheric pressure to a target pressure, Boyle's Law becomes:

$$N_{gait} * V_{piston} * P_{atm} + V_{PEA}(P_{atm}) * P_{atm} = V_{PEA}\left(P_{PEA,t}\right) * P_{PEA,t} \quad (1)$$

where N_{gait} is the number of gait cycles necessary to charge the PEA to the target pressure, V_{piston} is volume of air in the piston pump before compressing, $V_{PEA}(P_x)$ represents the volume of air inside the PEA when the gas pressure is P_x, $P_{PEA,t}$ is the unknown target pressure in the PEA that still needs to be determined (see Equation 12), and P_{atm}=101.3 kPa is atmospheric pressure.

2) Using the charged PEA to pressurize the FREE that was originally deflated and at atmospheric pressure up to the desired actuation pressure of 308.2 kPa (30 psig), Boyle's Law can be stated for this charging process as:

$$V_{FREE}(P_{atm}) * P_{atm} + V_{PEA}(P_{PEA,t}) * P_{PEA,t}$$

$$= V_{FREE}(P_{FREE,f}) * P_{FREE,f} + V_{PEA}(P_{PEA,f}) * P_{PEA,f} \quad (2)$$

where $V_{FREE}(P_x)$ represents the volume of air inside the FREE when the gas pressure is P_x. Due to equilibrium, the final pressure in the PEA and FREE should be equal, i.e., $P_{FREE,f} = P_{PEA,f} = 308.2$ kPa.

In addition, several physical constraints should hold for this system:

1) The maximum pressure that can be delivered to the PEA was constrained by the maximum pressure that can be generated from the piston pump. This maximum pressure, $P_{pump,max}$, was correlated with the maximum force applied to the piston pump, which can be approximately estimated to be half the user's body weight. In this case, the bubble pressure of the PEA, $P_{PEA,bubble}$, cannot be greater than $P_{pump,max}$; otherwise, no expansion bubble will develop in the PEA:

$$P_{PEA,bubble} \leq P_{pump,max} \approx \frac{\frac{1}{2}F_{bodywieght}}{\pi\left(\frac{d_{bore}}{2}\right)^2} + P_{atm} \quad (3)$$

where $P_{pump,max}$ is the maximum pressure that can be generated from the piston pump, $F_{bodywieght}$ is user's body weight, A_{piston} is the cross-sectional area of the piston head, d_{bore} is the diameter of the piston shaft, P_{atm} is the atmospheric pressure.

2) Since the PEA outputs a nearly constant fill pressure, $P_{PEA,fill}$, when charged and discharged, $P_{PEA,fill}$ should be greater than the final state pressure of 308.2 kPa. Otherwise, the bubble would still exist in the PEA at the final stage and the strain energy would not be efficiently transferred. At the beginning of design, we did not know the fill pressure of the PEA since the dimensions of PEA were undermined, so we would like to calculate the target pressure and find a PEA with fill pressure close to but smaller than this pressure. In addition, the target pressure should not be greater than the bubble pressure of the PEA when charged [65]:

$$308.2\ \text{kPa} < P_{PEA,fill} \leq P_{PEA,t} < P_{PEA,bubble} \quad (4)$$

3) Moreover, the stroke length was correlated with the comfort of the crutch user. We conducted an unpublished pilot study and determined that a stroke length higher than 2.54 cm (1 inch) was not preferred. In this case, we constrained the stroke length to no greater than 2.54 cm

$$h_{stroke} \leq 2.54\ cm \quad (5)$$

3.2.3 Determination of the design parameters

We aimed to determine design parameters that minimized the number of crutch gait cycles to store enough pressurized air in the PEA such that it could be used to charge the FREE to the desired actuation pressure of 308.2 kPa. Equations that we developed in the previous section characterizing charging processes were utilized. Key design parameters included the stroke length, bore diameter of the piston pump, and the specification of the PEA.

Combining Equations (1-2) and solving for the number of gait cycles needed to achieve the target PEA pressure, provided an expression that was a function of some design parameters.

$$N_{gait} = \frac{[V_{FREE}(P_{FREE,f})*P_{FREE,f}+V_{PEA}(P_{PEA,f})*P_{PEA,f}-V_{PEA}(P_{\text{atm}})*P_{atm}-V_{FREE}(P_{atm})*P_{atm}]}{V_{piston}*P_{atm}}$$

$$= \frac{[C_{FREE}(308.2\ kPa)-C_{FREE}(101.33\ kPa)+C_{PEA}(308.2\ kPa)-C_{PEA}(101.33\ kPa)]}{\pi\left(\frac{d_{bore}}{2}\right)^2*h_{stroke}*(101.33\ kPa)} \quad (6)$$

where we define capacitance as $C_x(P_x) = V_x(P_x) * P_x$. The term $C_{FREE}(308.2\ kPa) - C_{FREE}(101.3\ kPa)$ is only correlated with features of a given FREE.

In this case, to minimize the number of gait cycles, the first two conditions are:

Condition 1: $Minimize[C_{FREE}(308.2\ kPa) - C_{FREE}(101.3\ kPa)]$

Condition 2: $Maximize[(d_{bore})^2 * h_{stroke}]$

which is derived from $Maximize[\ \pi\left(\frac{d_{bore}}{2}\right)^2 * h_{stroke} * (101.33kPa)]$.

In addition, to make sure that the PEA can charge the FREE to 308.2 kPa, Equation (2) should also be satisfied:

Condition 3: $C_{PEA}(P_{PEA,f}) = C_{FREE}(308.2\ kPa) - C_{FREE}(101.3\ kPa) + C_{PEA}(308.2\ kPa)$

Moreover, physical constraints in the system should be satisfied. Our selection of the bore diameter of the piston shaft is related to the maximum pressure that can be generated in the system. Rearranging Equation (3), we get the expression with regard to the upper limit of the bore diameter of the piston shaft:

Condition 4: $$d_{bore} \leq 2\sqrt{\frac{\frac{1}{2}F_{bodywieght}}{\pi(P_{PEA,bubble} - P_{atm})}}$$

From Equations (3-4), we obtain relationship between characteristic pressure features of the PEA and the maximum pressure that can be generated from the piston pump to charge the PEA:

Condition 5: $$308.2\ \text{kPa} < P_{PEA,fill} \leq P_{PEA,target} \leq P_{PEA,bubble} \leq \frac{\frac{1}{2}F_{bodywieght}}{\pi\left(\frac{d_{bore}}{2}\right)^2} + P_{atm}$$

Equation (5) should also hold such that

Condition 6: $$h_{stroke} \leq 2.54\ cm$$

As the result, we have decoupled the optimization problem into six mathematical expressions that need to be satisfied, containing key design parameters (Conditions 1-6).

For Condition 1 to hold, the P-V relationship of a typical PEA was explored (Figure 3.6b). The volume of the PEA only goes through a small change before reaching the bubble pressure. After reaching the bubble pressure, a large bubble will be formed in the PEA and continue to propagate before the PEA reaches maximum volume. In this case, we would like to fabricate a PEA with a bubble pressure higher than 308.2 kPa to minimize the difference between $C_{PEA}(308.2\ kPa)$ and $C_{PEA}(101.3\ kPa)$. Combined with Condition (5), therefore, the bubble pressure in the PEA had to be between 308.2 kPa and the target PEA pressure.

$$308.2\ kPa < P_{PEA,bubble} \leq \frac{\frac{1}{2}F_{bodyweight}}{\pi\left(\frac{d_{bore}}{2}\right)^2} + P_{atm} \quad (7)$$

To satisfy Condition 2, we would like to maximize the volume of the piston pump. However, with increasing bore diameter, the maximum pressure that can be generated from the piston pump would be reduced. In this case, combining Conditions 2, 4 and 6, we identify the possible maximum value for the stroke length and bore diameter that satisfy:

$$h_{stroke} = 2.54\ cm \quad (8)$$

$$d_{bore} = 2\sqrt{\frac{\frac{1}{2}F_{bodyweight}}{\pi(P_{PEA,bubble} - P_{atm})}} \quad (9)$$

The latter of which is depend upon bodyweight and target pressure in the PEA.

For Condition 3, on the right side of the equation, the term $C_{FREE}(308.2\ kPa) - C_{FREE}(101.33\ kPa) + C_{PEA}(308.2\ kPa)$ could be experimentally determined. Tests were conducted to measure the volume of the FREE actuator at 308.2 kPa using a pressure transducer (PX309, Omega Engineering, Inc. Stamford, CT) and a volumetric flow meter (SFAB-10U-HQ6-2SA-M12, Festo Corp., Hauppauge, NY). In addition, by selecting a PEA with a bubble pressure greater than 308.2 kPa (Equation (7)), the term $C_{PEA}(308.2\ kPa)$ is nearly negligible.

$$C_{PEA}\left(P_{PEA,t}\right) = C_{FREE}(308.2\ kPa) - C_{FREE}(101.33\ kPa) + C_{PEA}(308.2\ kPa)$$
$$= \int_{t_{inital}}^{t_{final}} V_{measured}\,(t) * P_{measured}(t)dt - \pi\left(r_{FREE,atm}\right)^2 * L_{FREE,atm} \quad (10)$$

where $V_{measured}\,(t)$ is the measured volume calculated from the flow meter at time t, $P_{measured}(t)$ is the measured pressure from the pressure transducer at time t, $r_{FREE,atm}$ and $L_{FREE,atm}$ are the radius and the length, respectively, of the FREE at atmospheric pressure.

On the left side of the Equation (10), $C_{PEA}\left(P_{PEA,t}\right) = V_{PEA}\left(P_{PEA,t}\right) * P_{PEA,t}$. When the PEA was inflated, the wall thickness of the elastomer material became very thin. In this case, the cross-sectional

diameter of the expanded PEA was close to the inner diameter of the shroud constraining the PEA, and the length of bubbled PEA was also constrained by the length of available space inside the crutch shaft:

$$C_{PEA}(P_{PEA,t}) = V_{PEA}(P_{PEA,t}) * P_{PEA,t} \cong \pi\left(\frac{ID_{shroud}}{2}\right)^2 * L_{shaft} * P_{PEA,t} \quad (11)$$

where ID_{shroud} is the inner diameter of the crutch shaft, L_{shaft} is the available length inside the crutch shaft.

Consequently, combining Equations (10-11), we get

$$P_{PEA,t} = \frac{C_{PEA}(P_{PEA,t})}{\pi\left(\frac{ID_{shroud}}{2}\right)^2} = \frac{\int_{t_{inital}}^{t_{final}} V_{measured}(t) * P_{measured}(t)dt - \pi\left(r_{FREE,o}\right)^2 * L_{FREE}}{\pi\left(\frac{ID_{shroud}}{2}\right)^2 * L_{PEA,max}} \quad (12)$$

Experiments were conducted to measure the volume of the FREE at 308.2 kPa. $P_{PEA,t}$ was calculated to be 360.1 kPa using equation (12). In this case, to satisfy condition 5, we would like to select a PEA with bubble pressure greater than 360.1 kPa and fill pressure close to yet smaller than 360.1 kPa.

Due to lack of an analytical relationship between the characteristic pressures and the size of the elastomer tube, we fabricated several short PEAs with a length of 5 cm using off-the-shelf elastomer tubes of different dimensions to experimentally determine their bubble pressure and fill pressure (Table 3.1). A transparent shroud made of polyvinyl chloride (PVC) with an inner diameter of 2.54 cm and thickness of 0.39 cm was used to prevent the PEA from over expansion. Shop air with a pressure regulator was used as the power source, a pressure transducer (PX309, Omega Engineering, Inc. Stamford, CT) was used to monitor the pressure inside the PEA, and a micro-controller (Arduino UNO, Arduino Inc, New York City, NY) was used to collect time-series pressure data. During the experiment, the pressure was gradually increased in the PEA. Once it bubbled, the air supply was quickly turned off. The bubble pressure was identified by the peak pressure point and the fill pressure was identified as the local minima after the peak. Both pressures were averaged for three trials per sample PEA and were recorded in Table 3.1. Consequently the selected rubber tube (natural latex rubber, inner diameter: 0.32 cm, and outer diameter: 0. 80 cm) had a bubble pressure of 406.7 kPa and fill pressure of 342.6 kPa, which is greater

than 308.2 kPa and close to the target pressure of 360.1 kPa. The PEA for the energy storage system was then fabricated from this tube with a length of 20 cm.

The piston bore diameter was determined by plugging the value of $P_{PEA,bubble}$ into Equation (10). For the design of the PEC modified from a pair of Lofstrand crutches (Medline Forearm Crutches, Medline Industries, Inc., Mundelein, IL), the minimum user's height can be 152 cm (5 ft) [66]. In this case, a minimal body weight of 43.3 kg, according to the height-weight ratio chart from [67], was used to calculate the bore diameter.

$$d_{bore} = 2\sqrt{\frac{\frac{1}{2}(F_{bodywieght})}{\pi(P_{PEA,bubble}-P_{atm})}} \qquad (13)$$

Thus, using Equation (13), the bore diameter was determined to be 3.05 cm and a wall thickness of 1.27 mm was selected for all components. Finite element analysis (Creo Simulate 3.0, PTC Inc., Needham, MA) was conducted to estimate the von Mises stress in the components made of Aluminum 6061 when a force of 556 N (125 lb), which is the weight capacity of the Medline forearm crutches, was applied (Figure 3.8) [66]. A safety factor of 10 was achieved with this design.

Moreover, the number of gait cycles to reach the target pressure of the PEA that could then fully charge the FREE was calculated to be 30, using Equation (6).

3.3 BENCH-TOP TESTING OF THE PNEUMATIC ERGONOMIC CRUTCHES

3.3.1 Overview

Bench top testing was conducted to evaluate the performance of the energy harvesting system and the energy storage system. The PEA was first charged with the piston pump to a final pressure close to the target pressure of 360.1 kPa and the pneumatic sleeve orthosis was then charged using the air stored in the PEA in each PEC. We expected a smooth expansion of the PEA upon pressurization, without occurrence of a bubble in the distal end of PEA stopping the expansion of the remaining section. We

further expected a bubble pressure of 406.7 kPa in both PEAs and a final equilibrium pressure of 308.2 kPa in both sleeve orthoses. In addition, the number of crutch gait cycles used to reach the PEA to a steady-state should be close to 30 for both crutches. Furthermore, given the weight of the PEC user in this bench-top test to be 65 kg, the theoretical maximum pressure, $P_{pump,max}$, that can be generated from the piston pump was determined to be around 537.5 kPa using Equation (3):

$$P_{pump,max} \approx \frac{\frac{1}{2}F_{bodywieght}}{\pi\left(\frac{d_{bore}}{2}\right)^2} + P_{atm} = \frac{\frac{1}{2}\times 65\ kg \times 9.8\frac{N}{kg}}{\pi\left(\frac{3.05\ cm}{2}\right)^2} + 101.3\ kPa = 537.5\ kPa$$

3.3.2 Data collection

The pressures in the PEA and FREE were measured using two pressure transducers (PX309, Omega Engineering, Inc. Stamford, CT). A micro-controller (Arduino UNO, Arduino Inc, New York City, NY) was used to record the time-series pressure data. The number of gait cycles used to charge the PEA to just beyond the target pressure was counted.

3.3.2 Testing protocol

The PEC was originally set at locking mode, with the PEA and FREE both un-actuated. The PEC was repeatedly loaded such that the piston pump was completely compressed simulating multiple gait cycles. The number of compression cycles of the piston pump to achieve the target pressure just beyond 360.1 kPa after bubble formation was recorded. After the pressure in the PEA reached beyond the target pressure, the switch was then toggled to the charging mode to let the air stored in the PEA to charge the FREE. After the system reached an equilibrium of pressure in the PEA and FREE, the switch was then set to the discharging mode to relieve the pneumatic sleeve orthosis. Such protocol was repeated for three times. These transducers were attached on the left crutch first and then moved to measure the pressure in the PEA and FREE on the right PEC, following the same protocol for another three times.

3.3.3 Data processing

Collected data were processed using MATLAB (R2016a, Math Works, Inc. Natick, MA.). The bubble pressure, the fill pressure of the PEA, as well as the final pressure in the FREE were calculated from the time-series pressure data.

3.3.4 Results

The PEA was expanded smoothly as charged by the piston pump and was able to charge the sleeve orthosis to around 308.2 kPa. The PEA in the left and right PEC exhibited an averaged bubble pressure of 412.6 kPa and 411.5 kPa, and averaged fill pressure of 337.3 kPa and 338.2 kPa, respectively (Table 3.2-3.3). We were able to charge the left and right PEA to a final pressure of 357.7 kPa and 350.5 kPa before using them to charge the sleeve orthosis. The average number of gait cycles needed to reach this pressure was 38 for both crutches. The pneumatic sleeve orthosis reached 310.1 kPa in the left crutch and 307.9 kPa in right the crutch. The pressure-time plot for one trial was presented (Figure 3.9).

3.3.5 Discussion & Conclusion

Results from the bench top testing preliminarily validated the performance of the energy storage system and the energy harvesting system. Both PEAs expanded fully and smoothly in the crutch shaft, without the occurrence of a second inflation location. Their bubble pressures (412.6 kPa and 411.5 kPa) were slightly higher, while the fill pressures (337.3 kPa and 338.2 kPa) were slightly smaller than the measured bubble and fill pressure in the sample PEA ($P_{PEA,bubble}$ = 406.7 kPa, $P_{PEA,fill}$ = 342.6 kPa). Such discrepancies could be due to the difference in the length of PEA, changes in material property due to manufacturing defects or material wear. In addition, both pneumatic sleeve orthoses reached beyond 308.2 kPa with charged PEAs. However, the number of gait cycles to reach the target pressure in the PEA, 38 for both crutches, was higher than the theoretical value of 30. Leaks in the piston pump, inefficiency of the check valves, or energy loss during the discharging of the PEA might have caused such increase in

the number of gait cycles. Furthermore, the extra gait cycles could also be due to not being able to charge the PEA to the theoretical target pressure of 360.1 kPa, even after 38 gait cycles, as the maximum fill pressures were only 357.7 kPa and 350.5 kPa. It implied that the PEA might be too long such that it was not charged to its maximum volume after these amount of gait cycles, which explained that the final pressure in the PEA did not increase dramatically beyond the fill pressure. In this case, we would need to re-examine the derivations and build a more accurate model describing these charging processes. Nevertheless, the current system was demonstrated to satisfy our initial design objectives, and we would still like to keep such extra length in the PEA so that it could potentially store even more pressure energy.

3.4 HUMAN SUBJECT TESTING OF THE PNEUMATIC ERGONOMIC CRUTCHES

3.4.1 Overview

To further evaluate the performance of the pneumatic ergonomic crutches and validate the effectiveness of the shock absorption, six healthy able-bodied subjects will be recruited to perform swing-through crutch gait with the PEC, traditional Lofstrand crutches (Medline Forearm Crutches, Medline Inc, Northfield, IL) and a pair of commercially available spring-loaded crutches (Ergobaum 7G Foldable Ergonomic Crutches, Ergoactives LLC, Miami, FL) (Figure 3.1, 3.5a). Based on the effect of a previously designed spring-loaded crutch [33], we hypothesized that the piston pump would result in a reduced rate of GRF rise and a reduced magnitude of GRF at 2.5% and 5% of the crutch gait cycle, compared with traditional Lofstrand crutches. In addition, due to damping features induced by compressible air in the piston pump, we further hypothesized that the PEC would remain at a similar level of peak resultant GRF compared with traditional Lofstrand crutches.

3.4.2 Data collection

Pressure in the PEA and FREE will be collected as the subject practices swing-through gait with PEC as well as in gait trials with the PEC, using two pressure transducers (PX309, Omega Engineering, Inc. Stamford, CT) attached to the PEC on the dominant side near the crutch neck. The pressure data will be recorded by an external ADC board (USB-2533, Measurement Computing Corp., Norton, MA) synched with the motion capture system.

Crutch kinematics, ground reaction forces on the crutch tip, and pressures in the PEC will be collected during the test. Crutch kinematic data will be collected at 100 fps using a 6-camera motion capture system (Oqus-500, Qualisys North America, Inc. Deerfield, IL) and a 6-marker crutch model will markers placed at medial and lateral sides of the crutch neck, anterior and posterior sides of the mid shaft, and medial and lateral sides of the crutch tip (Figure 3.10a). In addition to crutch markers, heel and toe markers will also be placed on both feet at the calcaneus and second metatarsal head, respectively, to identify gait events. The ground reaction forces on the crutch tip on the dominant side will be recorded by a force plate (BP600900, AMTI, Watertown, MA) embedded at the center of the walkway (Figure 3.10b). Subject commentaries regarding the Borg rating of perceived exertion [61] of finishing the walking trial, and the perceived discomfort in upper extremities will also be recorded throughout the data collection.

3.4.3 Testing protocol

After signing the informed consent form, the height, weight and forearm girth will be measured and recorded for each subject. Before data collection trials, each subject will be required to practice with all three types of crutches for 30 min in total to become acclimated with performing the swing-through crutch gait on a walkway, under the instruction given on [4]. The length of each pair of crutches will be adjusted based on the instruction given on [3] for each subject. They will also be instructed to only place the dominant crutch tip, and no feet, on the force plate embedded at the center of the walkway. A unique

starting location will be additionally marked for each subject such that the dominant crutch tip will always land on the fore plate during the second or the third crutch gait cycle.

Additional protocol will be used when the subject practices with the PEC and the pressure in the PEA and FREE will be recorded in the whole practice process. The PEC will be initially set to locking mode with the PEA and FREE both unpressurized. As the subject performs swing-through crutch gait, pressure will be accumulating in the PEA. When the PEA pressure reaches a steady state. The subject will then be instructed to push the toggle switch to charging mode to actuate the pneumatic sleeve orthosis with air stored in the PEA. After reaching a comfortable level constriction pressure on the forearm, the subject then pushes to switch back to locking mode and continue to practice with the PEC to pressurize the PEA with the actuated pneumatic sleeve orthosis. Pressure in the steady state of the PEA and the user-selected actuation pressure of the FREE will be recorded. At the end of practice session, the user will push the toggle switch to discharging mode to exhaust pressure in the FREE. However, the PEA will stay fully charged inside the PEC.

During the data collection trials, the subject will be asked to walk over the 6m walkway with three types of crutches: traditional Lofstrand crutches, spring-loaded crutches, and the PEC. The testing order will be randomized for each subject. In each trial, the subject will first stand behind the marked starting location, hold the crutch up in the air. Once instructed to start, the subject will perform swing-through gait over the walkway and stop when passing an end marker. To minimize fatigue and upper extremity discomfort, the subject will then hold the crutches up and walk back to the starting location, getting ready for the next trial. At least three good trials will be collected for each testing condition. A good trial is defined as: 1) the subject performs a symmetric swing-through gait pattern where both feet take off and strike at a similar time, 2) the subject successfully lands the dominate crutch tip, and no feet, on the force plate, 3) no missing markers for more than 20 ms when the subject passes through the force plate, and 4) force plate data and additional pressure data are successfully recorded. A seated rest of at least 1 min will

be provided after each trial, and a seated rest of at least 5 min will be offered when finishing one test condition. Subjects will be additionally asked to evaluate the Borg rating of perceived exertion after each trial and will also be asked to describe the discomfort level of their upper extremity joints after finishing one testing condition.

Additional protocols will also be used in trials walking with the PEC to simulate a steady state of the PEC, in which the PEA is charged to steady state and the pneumatic sleeve orthosis is pressurized to a comfortable level. At the end of the crutch gait acclimation stage, the PEA in the PEC should be fully charged while the sleeve orthosis is unactuated. Before walking with the PEC, the subject will don the PEC and the pneumatic sleeve orthosis will be charged to the user-selected actuation pressure (recorded in the acclimation stage) using shop air, while keeping the PEA in a steady state. The protocol for the walking trail is the same as other test conditions, except pressure from the FREE and PEA will be additionally collected.

3.4.4 Data processing

Crutch kinematics and GRFs in the gait cycle on the force plate will be post-processed using Qualisys Track Manager (V2.13, Qualisys North America, Inc. Deerfield, IL) and MATLAB (R2016, Math Works, Natick, MA). The evaluated gait cycle from the first crutch strike on the force plate to the next crutch strike on the walkway will be extracted from each trial. A force threshold of 10 N will be used to identify the initial crutch strike on the force plate, the vertical height of the medial crutch tip marker at this moment will be recorded and used to identify the next crutch strike event on the walkway. Crutch kinematics data will be processed using Qualisys Track Manager and MATLAB software. The longitudinal displacement of the piston pump in the PEC and spring-loaded crutch tip Ergobam crutches will be calculated. Ground reaction force data collected from the force plate will be processed in MATLAB. To assess the effect of shock absorption, the maximum resultant GRF increasing rate, magnitude of resultant GRF at 2.5% and 5% of the crutch gait cycle, and the peak magnitude of the resultant GRF will be

determined for each trial and averaged per test condition. Multivariate analysis of variance (MANOVA) will be done to these kinetic parameters.

3.5 CONCLUSION

We have designed a pneumatic ergonomic crutch (PEC) consisting of a pneumatic sleeve orthosis, an energy harvesting spring-loaded piston pump, a pneumatic elastomeric accumulator (PEA), and a pneumatic control system. The pneumatic sleeve orthosis has been previously validated to improve the wrist posture, share loads, and redistribute palmar pressure for crutch users. The spring-loaded piston pump was attached to the crutch tip, provided shock absorption, and collected pneumatic energy during the crutch gait during crutch gait. The PEA was integrated into the crutch shaft and stored the energy in the crutch system, which could be used for actuation of the pneumatic sleeve orthosis through the control system. The processes of charging the PEA using the piston pump and charging the pneumatic sleeve orthosis using the PEA were modeled. Analytical expressions characterizing the charging processes and physical constraints were developed. The design parameters for the piston pump and PEA were optimized to minimize the number of crutch gait cycles to fully charge the pneumatic sleeve orthosis and maximize the capacity of energy storage based on these expressions. A bench-top testing of the PEC was conducted and preliminarily results demonstrated the performance of the PEC in terms of energy harvesting, energy storage, and pressurization of the pneumatic sleeve orthosis. Human subject testing will be conducted to test the PEC on healthy adult subjects to not only evaluate the system performance, but also to validate the effectiveness of shock absorption induced by the piston pump on crutch gait. Subjects will perform swing-through crutch gait with a pair of traditional Lofstrand crutches, commercially available spring-loaded crutches, and the pneumatic ergonomic churches. Crutch kinematics and ground reaction forces at dominant crutch tip will be measured, and the resultant GRF will be analyzed. The maximum resultant

GRF increasing rate, magnitude of resultant GRF at 2.5% and 5% of the crutch gait cycle, the peak magnitude of the resultant GRF will be calculated.

In conclusion, we have designed and fabricated a pair of pneumatic ergonomic crutches that was able to harvest pneumatic energy during the crutch gait, store the energy and use the energy to power a pneumatic sleeve orthosis. Bench-top testing was conducted and preliminarily validated the performance of the PEC in term of charging the pneumatic sleeve orthosis to a desired pressure. Human subject testing will also be conducted in the future to evaluate the effectiveness of shock absorption of the PEC.

3.6 FIGURES

(a) (b)

Figure 3.1. (a) Key components of a pair of standard Lofstrand crutches (Medline Industries, Inc., Northfield, Illinois), (b) Spring-loaded Lofstrand crutch (Ergobaum forearm crutches, Ergoactives Orthopedic Device Company, Hallandale Beach, FL).

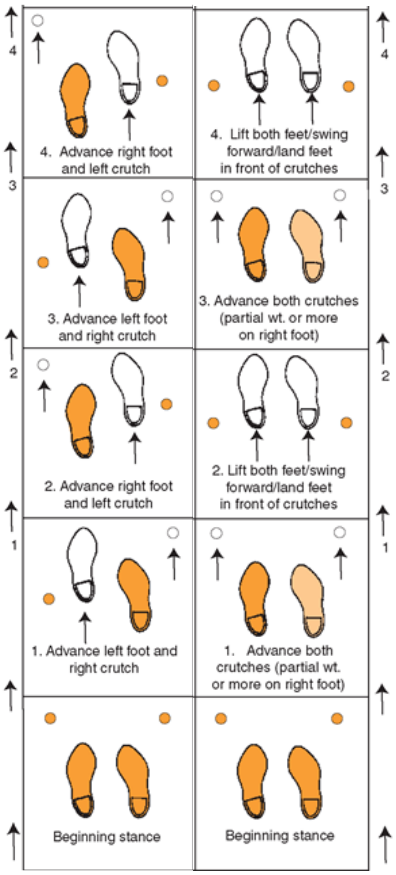

(a) (b)

Figure 3.2. Crutch gait pattern: (a) reciprocal gait, and (b) swing-through gait [4]

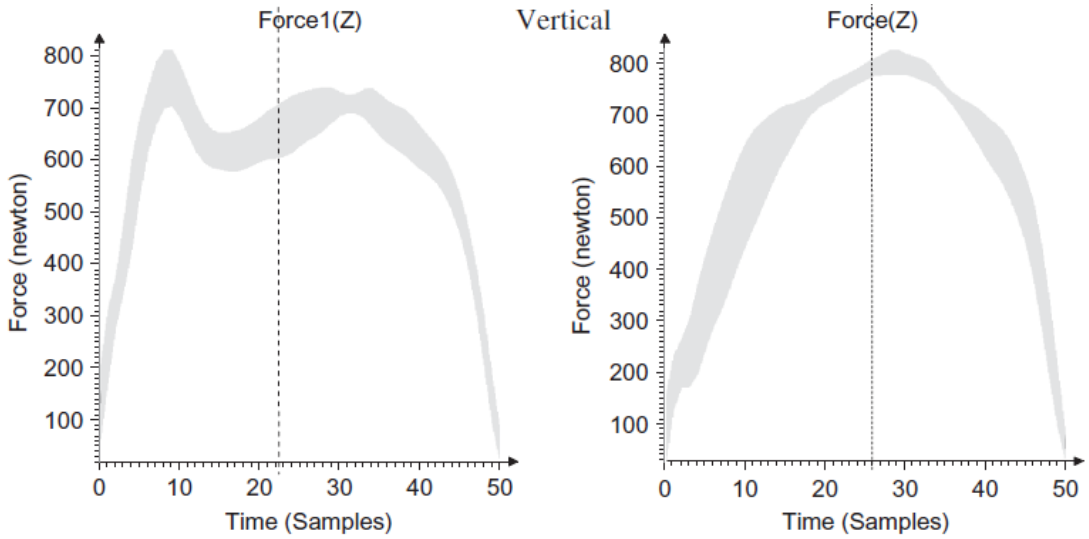

Figure 3.3. Reproduction of Figure 3 from [30]. Vertical ground reaction forces for subject 1 while using traditional Lofstrand crutch (left) and spring-loaded crutch (right). Time was normalized to 50 frames. Shaded areas = ±1 standard deviation. The two vertical dashed lines mark mid-stance time.

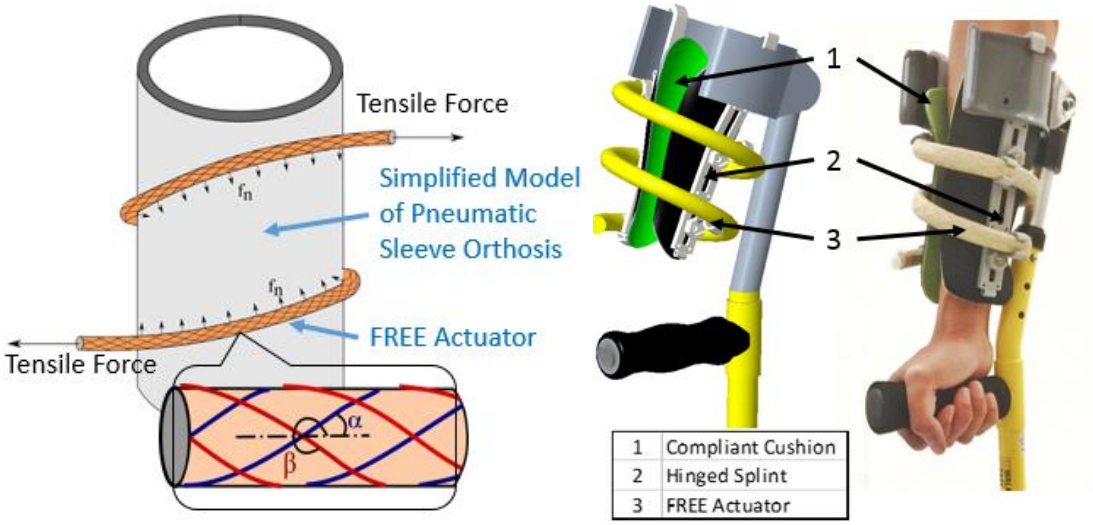

(a) (b)

Figure 3.4. (a) Illustration of FREE Actuator and generation of constriction force in coiled configuration [63] [62], (b) CAD and prototype of the Pneumatic Sleeve Orthosis

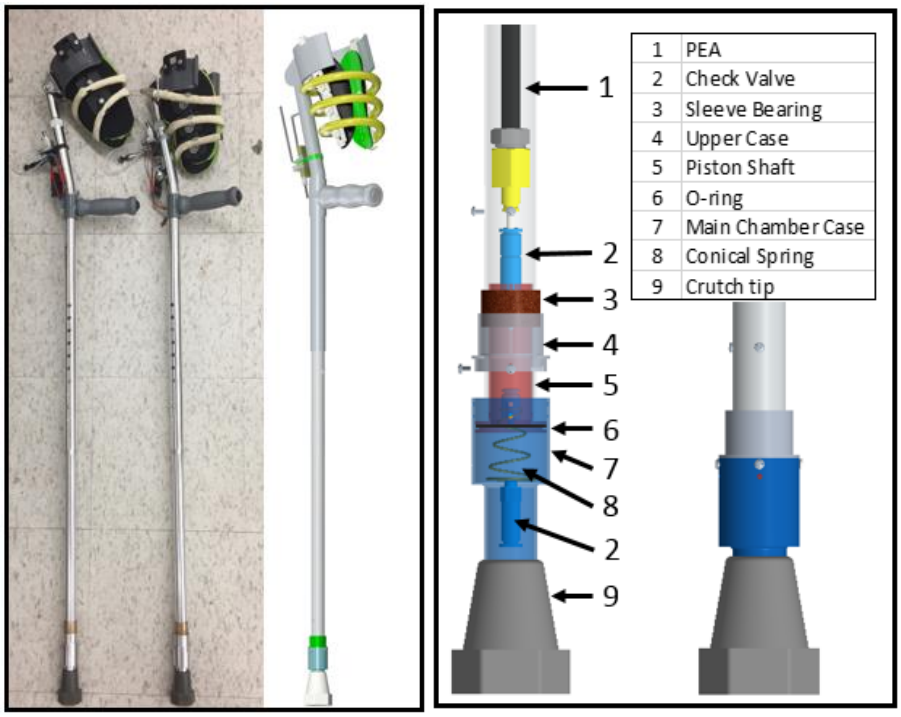

(a) (b)

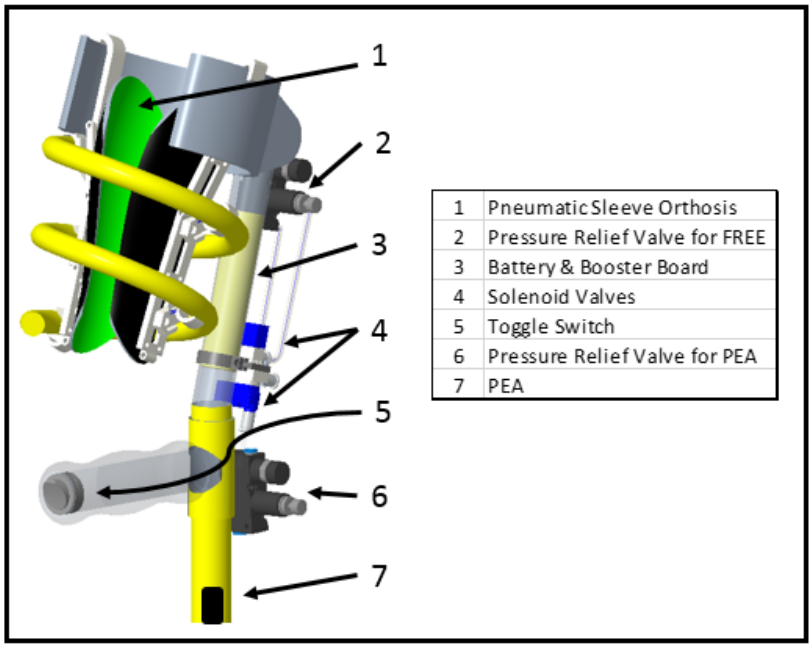

(c)

Figure 3.5. (a) CAD and prototype of PEC; (b) CAD design of the piston pump, exploded view on the left side and assembly view on the right side; (c) Pneumatic sleeve orthosis and integration of pneumatic control system components into crutch neck and crutch handle.

(a)

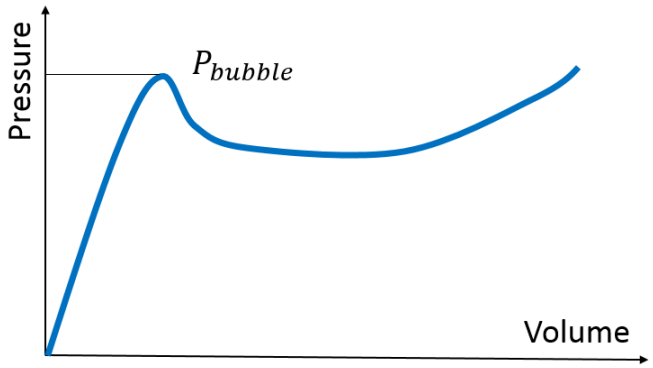

(b)

Figure 3.6. (a) Prototype of PEA in a rigid shroud with a bubbled section, (b) Reproduction of a typical pressure-volume relationship of PEA [53]

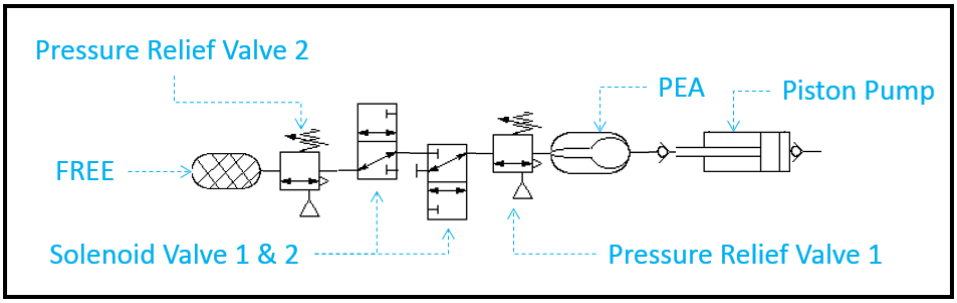

(a)

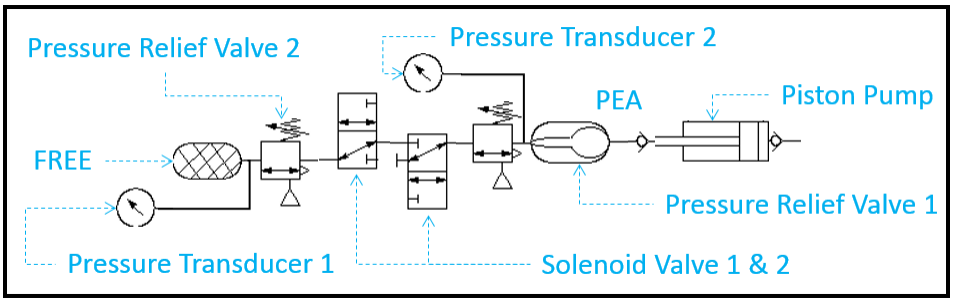

(b)

Figure 3.7. Pneumatic circuit designs (a) pneumatic circuit for the pneumatic ergonomic crutches, and (b) pneumatic circuit diagram for bench-top testing

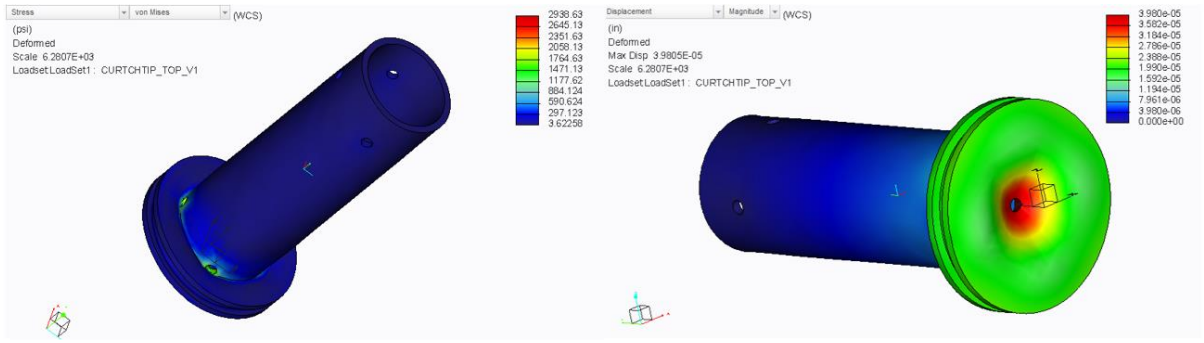

(a)

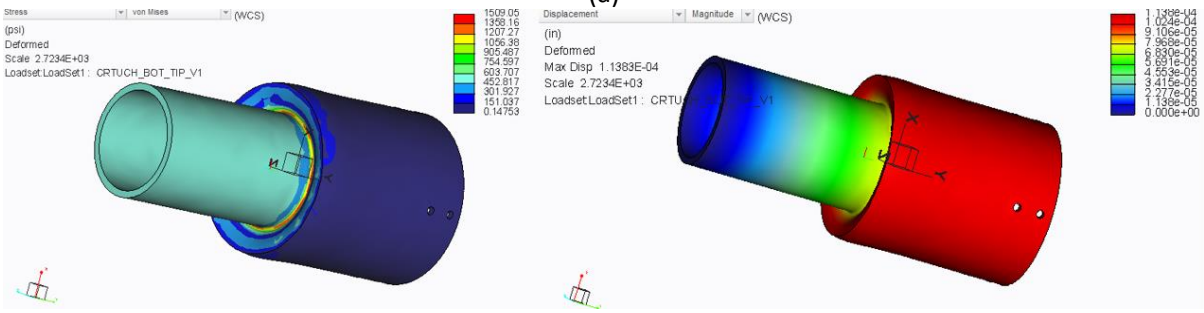

(b)

Figure 3.8. FEA of piston pump (a) Maximum stress of 20.3 MPa and maximum displacement 1.01E-3 mm, (b) maximum stress 10.4 MPa and maximum displacement 2.89E-3 mm when loaded.

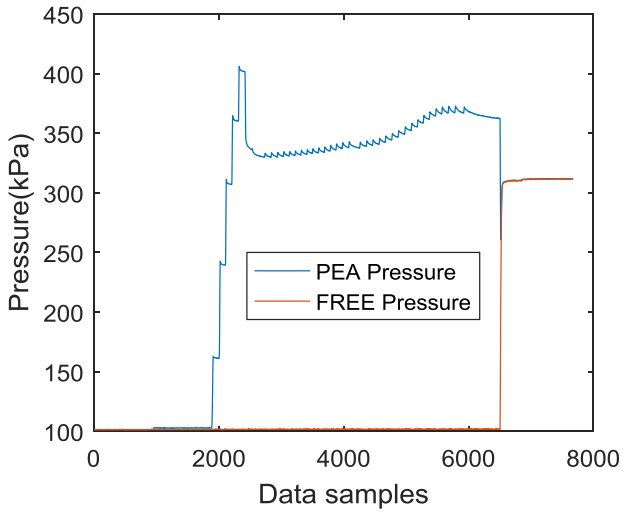

Figure 3.9. Pressure in FREE and PEA during bench-top testing of one trial

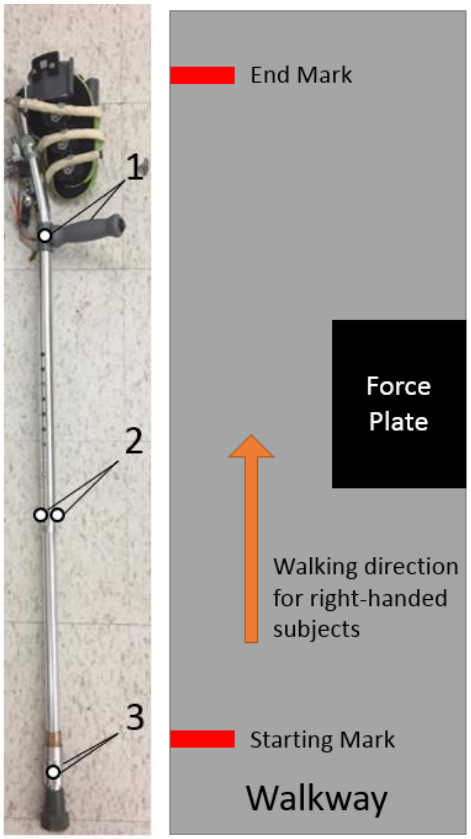

(a) (b)

Figure 3.10. Human subject testing (a) crutch maker model: 1) medial & lateral crutch handle markers, 2) anterior & posterior crutch shaft markers, and 3) medial & lateral crutch tip markers; (b) walkway with force plate embedded at center to the right.

Table 3.1. *PEA Specs and Bubble Pressure*

PEA ID	Material	ID (inch)	OD (inch)	Averaged Bubble Pressure (kPa)	Averaged fill Pressure (kPa)
1	Natural Latex Rubber	1/8	1/4	297.9	240.8
2	Natural Latex Rubber	5/32	9/32	327.1	274.4
3	Natural Latex Rubber	3/16	5/16	306.5	241.6
4	**Natural Latex Rubber**	**1/8**	**5/16**	**406.7**	**342.6**
5	Natural Latex Rubber	1/8	3/8	422.9	385.7
6	High-Flex Rubber	1/8	1/4	253.4	193.3
7	High-Temperature Silicon Rubber*	1/8	1/4	/	/

*: this accumulator did not exhibit a typical hyperplastic behavior when pressurized

Table 3.2. *Evaluation of the Energy Harvesting System and Energy Storage System in the Left Pneumatic Ergonomic Crutch*

Trail	PEA bubble pressure (kPa)	PEA fill pressure (kPa)	PEA final pressure (kPa)	FREE final pressure (kPa)	Number of gait cycles
1	406.3	339.1	362.3	311.6	40
2	404.8	338.6	348.9	308.1	36
3	426.6	334.2	361.9	310.6	37
Mean	412.6 ± 12.2	337.3 ± 2.7	357.7 ± 7.6	310.1 ± 1.8	38

Table 3.3. *Evaluation of the Energy Harvesting System and Energy Storage System in the Right Pneumatic Ergonomic Crutch*

Trail	PEA bubble pressure (kPa)	PEA fill pressure (kPa)	PEA final pressure (kPa)	FREE final pressure (kPa)	Number of gait cycles
1	410.9	337.1	345.2	306.8	38
2	411.5	335.1	353.4	307.9	36
3	412.1	342.4	352.9	309.1	40
Mean	411.5± 0.6	338.2 ± 3.8	350.5 ± 4.6	307.9 ± 1.2	38

CHAPTER 4: CONCLUSIONS

4.1 REVIEW OF FINDGINGS

4.1.1 Pneumatic sleeve orthosis

We have designed a pneumatic sleeve orthosis utilizing a soft pneumatic actuator and compliant splints to apply a comfortable constriction pressure to the forearm and thus establish a physical connection between the forearm and the crutch cuff. We have demonstrated its effectiveness of improving wrist posture, sharing wrist force, and reducing and redirecting palmar pressure while safely interacting with users of Lofstrand crutches. These effects were most significant in the more biomechanically taxing swing-through crutch gait. Peak and mean wrist extension angles, wrist extension ROM, and peak and mean ulnar deviation angles were significantly reduced, peak and mean crutch forces were significantly increased, and peak and mean palmar pressures were significantly decreased. Even though no statistically significant differences were identified in reciprocal gait trials, similar trends were observed from these results. In addition, a shift of pressure concentration away from the carpal tunnel region was observed with the use of the orthosis. Furthermore, a reduced perceived exertion was also recorded during crutch gait using Lofstrand crutches modified with the pneumatic sleeve orthosis.

4.1.2 Pneumatic ergonomic crutches

We also developed a pair of pneumatic ergonomic crutches (PEC) by modifying the traditional Lofstrand crutch to contain the pneumatic sleeve orthosis, an energy harvesting system, an energy storage system, and a pneumatic control system. We successfully harvested pneumatic energy from crutch gait cycles using a spring-loaded piston pump attached to the crutch tip. A pneumatic elastomeric accumulator (PEA) was integrated into the crutch shaft to store the collected air for the subsequent actuation of the pneumatic sleeve orthosis. Thus, the system was truly self-contained. Charging processes in the PEC were analytically derived and design parameters of the piston pump and the PEA were optimized. A theoretical

minimal number of crutch gait cycles of 30 was required to charge the PEA such that it can be used to actuate the sleeve orthosis to 308.2 kPa. Bench-top testing was conducted and preliminarily validated the performance of the PEC in term of energy harvesting, energy storing and charging capability. The PEC was able to collect and store energy effectively. However, due to energy losses and potential leaking in the system, it required 38 gait cycles to charge the pneumatic sleeve orthosis to be over 308.2 kPa.

4.2 EXPANSION ON THE DESIGN OF THE PNEUMATIC ERGONOMIC CRUTCHES

The design of the pneumatic ergonomic crutches explored several innovative design concepts. In the design of the pneumatic sleeve orthosis, we investigated a new method of establishing a physical interface between the soft pneumatic actuator, the FREE actuator, and the object. Coiled around the forearm and fixed to both ends on the splint, the FREE generated a normal constriction force along its length to the forearm upon actuation, like an elephant trunk or a snake's body. Analytical and experimental work were done to analyze and quantify the constriction force generated by the coiled FREE [63]. Such interface could be applied in other applications where a normal force is required to be generated along the contour of an object. Moreover, through the design of the pneumatic ergonomic crutches, we have also built a miniature self-contained pneumatic system inside a pair of Lostrand crutches. Though small, the system contained a power source, an accumulator, an actuator and a control system. We utilized a minimal profile design such that the piston pump was attached to the crutch tip, the pneumatic elastomeric accumulator (PEA) was hidden inside the crutch shaft, and most electronic components were also integrated into the hollow shaft of the crutches. In additional, by harvesting energy from the piston pump and store the energy in the PEA, this pneumatic system did not require external pneumatic power supply. In this case, we have also successfully exploited the energetics of harvesting pneumatic energy from crutch gait, utilizing the advantages of the fluid system.

Human subject testing of the pneumatic sleeve orthosis and pilot study on the PEC validated the benefits of establishing an interface between the forearm and the cuff, and providing shock absorption during the crutch gait biomechanically. These implications could be utilized in the design of more cost-effective ergonomic crutches. The current design of the PEC, due to integration of all pneumatic and electro-mechanical components, might be too complicated and not as cost-effective as other passive designs. Researchers from our group, including this author, have previously developed a pair of simple passive wrist orthosis [37] to improve the wrist posture and redirect palmar pressure using a 3D printed structure and a nylon band to provide a wrist support. Even though this device was not be able to share the load between the wrist and the forearm, it was able to provide a significant uniform reduction of wrist extension angle. In this case, passive ergonomic crutches with mechanisms that stabilize the forearm, support the wrist, and provide shock-absorbing might the most cost-effective solution to address the issues of wrist pain, strain, deformity, carpal tunnel syndrome and other injuries that are associated with long term crutch using [14-28].

Moreover, with the development of lower extremity exoskeletons such as ReWalk (ReWalk Robotics, Inc. Marlborough, MA) and Ekso Bionics (Ekso Bionics Holdings, Inc. Richimond, CA), people who could only use a wheelchair for locomotion in the past are now able to walk with crutches with the help from these wearable robotics. Even though their body weights are mainly supported by the exoskeletons, users still need crutches to stabilize themselves during locomotion or support themselves in the event of losing balance. In this case, there might be a growing need for ergonomic crutches for these exoskeletons users.

4.3 FUTURE WORK

Human subject testing will also be conducted in the future to evaluate the system performance and effectiveness of the shock absorption of the PEC among able-bodied subjects. Subjects will perform

swing-through gait over a 6m walkway with three types of crutches: traditional Lofstrand crutches, commercially available spring-loaded Lofstrand crutches, and the PEC. The ground reaction forces (GRFs) on the dominant crutch tip will be recorded by a force plate on the walkway, for 3 trials of each test condition. Crutch kinematics will also be collected using a 6-camera motion capture system.

To evaluate the effectiveness of the ground reaction forces, the maximum rate of the resultant GRF increase, the magnitude of the resultant GRF at 2.5% and 5% of the crutch gait cycle, and the peak resultant GRF magnitude will be calculated and averaged per test condition for each subject. MANOVA will be conducted on these parameters for all three conditions. We hypothesize the PEC will provide shock absorption without introducing an increase peak GRF magnitude. Specifically, we expect a reduced maximum rate of the resultant GRF increase and a reduced resultant GRF magnitude at 2.5% and 5% of the crutch gait cycle in spring-loaded Lofstrand crutches and the PEC compared with traditional Lofstrand crutches. We additionally hypothesize an increased peak resultant GRF magnitude in the spring-loaded Lostrand crutches compared with the PEC and the traditional Lofstrand crutches.

REFERENCES

[1] Kaye, H. S., Kang, T. & LaPlante, M.P. (2000). Mobility device use in the United States. Disability statistics report, (14). Washington, D.C.: U.S. Department of Education, National Institute on Disability and Rehabilitation Research.

[2] Joyce, B.M., Kirby, R.L. (1991). Canes, Crutches and Walkers. *Am Fam Physician, 43*(2), 535-542.

[3] Forearm Crutches (Canadian Crutches, Lofstrand Crutches, Elbow Crutches). (2002). Retrieved from http://www.qualitymedicalinc.com/forearm_crutches.htm

[4] Preparation for Crutch-Walking. Retrieved from http://what-when-how.com/nursing/body-mechanics-and-positioning-client-care-nursing-part-4/

[5] O'Sullivan, S., Schmitz, T.J. & Fulk, G. (2013). Physical Rehabilitation. Philadelphia, PA: F.A. Davis.

[6] Youdas, J. W., Kotajarvi, B. J., Padgett, D. J., & Kaufman, K. R. (2005). Partial weight-bearing gait using conventional assistive devices. *Archives of Physical Medicine and Rehabilitation*, *86*(3), 394–398. https://doi.org/10.1016/j.apmr.2004.03.026

[7] Haubert, L. L., Gutierrez, D. D., Newsam, C. J., Gronley, J. K., Mulroy, S. J., & Perry, J. (2006). A comparison of shoulder joint forces during ambulation with crutches versus a walker in persons with incomplete spinal cord injury. *Archives of Physical Medicine and Rehabilitation*, *87*(1), 63–70.

[8] Melis, E. H., Torres-Moreno, R., Barbeau, H., & Lemaire, E. D. (1999). Analysis of assisted-gait characteristics in persons with incomplete spinal cord injury. *Spinal Cord : The Official Journal of the International Medical Society of Paraplegia*, *37*(6), 430–439.

[9] Requejo, P. S., Wahl, D. P., Bontrager, E. L., Newsam, C. J., Gronley, J. K., Mulroy, S. J., & Perry, J. (2005). Upper extremity kinetics during Lofstrand crutch-assisted gait. *Medical Engineering and Physics*, *27*(1), 19–29.

[10] Slavens, B. A., Sturm, P. F., Bajournaite, R., & Harris, G. F. (2009). Upper extremity dynamics during Lofstrand crutch-assisted gait in children with myelomeningocele. *Gait and Posture*, *30*(4), 511–517.

[11] Slavens, B. A., Sturm, P. F., & Harris, G. F. (2010). Upper extremity inverse dynamics model for crutch-assisted gait assessment. *Journal of Biomechanics*, *43*(10), 2026–2031.

[12] Slavens, B. A., Bhagchandani, N., Wang, M., Smith, P. A., & Harris, G. F. (2011). An upper extremity inverse dynamics model for pediatric Lofstrand crutch-assisted gait. *Journal of Biomechanics*, *44*(11), 2162–2167.

[13] Noreau, L., Richards, C. L., Comeau, F., & Tardif, D. (1995). Biomechanical analysis of swing-through gait in paraplegic and non-disabled individuals. *Journal of Biomechanics*, *28*(6), 689–700.

[14] Koh, E. S. C., Williams, A. J., & Povlsen, B. (2002). Upper-limb pain in long-term poliomyelitis, *Quarterly Journal of Medicine, 95*(6), 389–395.

[15] Aljure, J., Eltorai, I., Bradley, W., Lin, J., & Johnson, B. (1985). Carpal tunnel syndrome in paraplegic patients. *Paraplegia*, *23*, 182–186.

[16] Pentland, E., Bscot, C., & Twomey, L. T. (1991). The weight-bearing upper extremity in women with long term paraplegia, *Paraplegia*, *29*(8), 521–530.

[17] Waring, W. P. 3Rd, & Werner, R. a. (1989). Clinical management of carpal tunnel syndrome in patients with long-term sequelae of poliomyelitis. *The Journal of Hand Surgery*, *14*(5), 865–869.

[18] Wiley, A. M. (1959). The carpal tunnel syndrome. *Postgraduate Medical Journal*, *35*(399), 30–33.

[19] Cobb, T.K., An. K.N., & Cooney., W.P. (1995). Externally Applied Forces to the Palm Increase Carpal Tunnel Pressure. *Journal of Hand Surgery, 20*(2), 181-185.

[20] Weiss, N.D., Gordon, L., Bloom, T., So, Y., Rempel., D.M. (1995). Position of the wrist associated with the loweest carpal-tunnel pressure: implication for splint design. *Journal of Bone & Joint Suregery, 77*(11), 1695-1699.

[21] Keir, P. J., Bach, J. M., & Rempel, D. M. (1998). Effects of finger posture on carpal tunnel pressure during wrist motion. *The Journal of Hand Surgery, 23*(6), 1004-1009.

[22] Gelberman, R. H., Hergenroeder, P. T., Hargens, A. R., Lundborg, G. N., & Akeson, W. H. (1981). The carpal tunnel syndrome. A study of carpal canal pressures. *Journal of Bone & Joint Surgery, 63*(3), 380-383.

[23] Goss, B. C., & Agee, J. M. (2010). Dynamics of Intracarpal Tunnel Pressure in Patients with Carpal Tunnel Syndrome. *The Journal of Hand Surgery*, *35*(2), 197–206.

[24] Brown, R. A., Gelberman, R. H., Seiler 3rd, J. G., Abrahamsson, S. O., Weiland, A. J., Urbaniak, J. R., ... & Furcolo, D. (1993). Carpal tunnel release. A prospective, randomized assessment of open and endoscopic methods. *Journal of Bone & Joint Surgery, 75*(9), 1265-1275.

[25] Palmer, K. T. (2003). Pain in the forearm, wrist and hand. *Best Practice & Research Clinical Rheumatology, 17*(1), 113-135.25

[26] Van Thulder, M., Malmivaara, A., & Koes, B. (2007). Repetitive strain injuries. *The Lancet, 369*(9575), 1815–1822.

[27] Chang, I. T., & Hohler, A. D. (2012). Bilateral radial nerve compression (crutch palsy): a case report, *Journal of Neurology & Neurophysiology, 3*(3), 10–11.

[28] Ginanneschi, F., Filippou, G., Milani, P., & Biasella, A. (2009). Ulnar nerve compression neuropathy at guyon ' s canal caused by crutch walking : case report with ultrasonographic nerve imaging. *Archives of Physical Medicine and Rehabilitation*, *90*(3), 522–524.

[29] Zhang, Y., Beaven, M., Liu, G., & Xie, S. (2013). Mechanical efficiency of walking with spring-loaded axillary crutches. *Assistive Technology, 25*(2), 111-116.

[30] Zhang, Y., Liu, G., Xie, S., & Liger, A. (2011). Biomechanical evaluation of an innovative spring-loaded axillary crutch design. *Assistive Technology, 23*(4), 225-231.

[31] Liu, G., Xie, S. Q., & Zhang, Y. (2011). Optimization of spring-loaded crutches via boundary value problem. *IEEE Transactions on Neural Systems and Rehabilitation Engineering, 19*(1), 64-70.

[32] Seeley, M. K., Sandberg, R. P., Chacon, J. F., Funk, M. D., Nokes, N., & Mack, G. W. (2011). Metabolic energy expenditure during spring-loaded crutch ambulation. *Journal of Sport Rehabilitation, 20*(4), 419-427.

[33] Segura, A., & Piazza, S. J. (2007). Mechanics of ambulation with standard and spring-loaded crutches. *Archives of Physical Medicine and Rehabilitation, 88*(9), 1159-1163.

[34] Parziale, J. R., & Daniels, J. D. (1989). The mechanical performance of ambulation using spring-loaded axillary crutches: a preliminary report. *American Journal of Physical Medicine & Rehabilitation, 68*(4), 192-195.

[35] Sala, D. A., Leva, L. M., Kummer, F. J., & Grant, A. D. (1998). Crutch handle design: effect on palmar loads during ambulation. *Archives of Physical Medicine & Rehabilitation*, *79*(11), 1473-1476.

[36] Smith, A. A. (1966). U.S. Patent No. 3,269,399. Washington, DC: U.S. Patent and Trademark Office.

[37] Farooq, D., Jahanian, O., Slavens, B. A., & Hsiao-Wecksler, E. T. (2016, August). Evaluation of a wrist orthosis on Lofstrand crutch-assisted gait. In *Engineering in Medicine and Biology Society (EMBC), 2016 IEEE 38th Annual International Conference of the* (pp. 5042-5045). IEEE.

[38] Kim, S., Laschi, C., & Trimmer, B. (2013). Soft robotics: a bioinspired evolution in robotics. *Trends in biotechnology*, *31*(5), 287-294.

[39] Ilievski, F., Mazzeo, A. D., Shepherd, R. F., Chen, X., & Whitesides, G. M. (2011). Soft robotics for chemists. *Angewandte Chemie*, *123*(8), 1930-1935.

[40] Mosadegh, B., Polygerinos, P., Keplinger, C., Wennstedt, S., Shepherd, R. F., Gupta, U., Shim, J., Bertoldi, K., Walk, J. C., & Whitesides, G. M. (2014). Pneumatic networks for soft robotics that actuate rapidly. *Advanced Functional Materials*, *24*(15), 2163-2170.

[41] Polygerinos, P., Lyne, S., Wang, Z., Nicolini, L. F., Mosadegh, B., Whitesides, G. M., & Walsh, C. J. (2013, November). Towards a soft pneumatic glove for hand rehabilitation. In Intelligent Robots and Systems (IROS), 2013 IEEE/RSJ International Conference on (pp. 1512-1517). IEEE.

[42] Bishop-Moser, J., & Kota, S. (2015). Design and modeling of generalized fiber-reinforced pneumatic soft actuators. *IEEE Transactions on Robotics*, *31*(3), 536-545.

[43] Bishop-Moser, J., Krishnan, G., & Kota, S. (2013, November). Force and moment generation of fiber-reinforced pneumatic soft actuators. In *Intelligent Robots and Systems (IROS), 2013 IEEE/RSJ International Conference* (pp. 4460-4465). IEEE.

[44] Bishop-Moser, J., Krishnan, G., & Kota, S. (2013). Force and hydraulic displacement amplification of fiber reinforced soft actuators. *Ann Arbor*, *1001*, 48109.

[45] Singh, G., & Krishnan, G. (2015, September). An isoperimetric formulation to predict deformation behavior of pneumatic fiber reinforced elastomeric actuators. In *2015 IEEE/RSJ International Conference on Intelligent Robots and Systems (IROS),* (pp. 1738-1743). IEEE.

[46] Bishop-Moser, J., Krishnan, G., Kim, C., & Kota, S. (2012, October). Design of soft robotic actuators using fluid-filled fiber-reinforced elastomeric enclosures in parallel combinations. In *2012 IEEE/RSJ International Conference on Intelligent Robots and Systems (IROS),* (pp. 4264-4269). IEEE.

[47] Tondu, B., & Lopez, P. (2000). Modeling and control of McKibben artificial muscle robot actuators. *IEEE Control Systems*, *20*(2), 15-38.

[48] Park, Y. L., Chen, B. R., Pérez-Arancibia, N. O., Young, D., Stirling, L., Wood, R. J., Goldfield, E.C., & Nagpal, R. (2014). Design and control of a bio-inspired soft wearable robotic device for ankle–foot rehabilitation. *Bioinspiration & biomimetics*, *9*(1), 016007.

[49] Shiraishi, M., & Watanabe, H. (1996). Pneumatic assist device for gait restoration. *Journal of Dynamic Systems, Measurement, and Control*, *118*(1), 9-14.

[50] Durfee, W. K., & Rivard, A. (2005). Design and simulation of a pneumatic, stored-energy, hybrid orthosis for gait restoration. *Journal of Biomechanical Engineering*, *127*(6), 1014-1019.

[51] Chin, R., Hsiao-Wecksler, E. T., Loth, E., Kogler, G., Manwaring, S. D., Tyson, S. N., Shorter, K.A., & Gilmer, J. N. (2009). A pneumatic power harvesting ankle-foot orthosis to prevent foot-drop. *Journal of Neuroengineering & Rehabilitation*, *6*(1), 19.

[52] Pedchenko, A., & Barth, E. J. (2009, October). Design and validation of a high energy density elastic accumulator using polyurethane. In *ASME Dynamic Systems and Control Conference* (Vol. 1, pp. 283-290).

[53] Cummins, J. J. (2016*). Characterization of a pneumatic strain energy accumulator: efficiency and first principles models with uncertainty analysis* (Doctoral dissertation). Vanderbilt University.

[54] Tucker, J. M. (2012). *Design and experimental evaluation of a high energy density elastomeric strain energy accumulator* (Doctoral dissertation). Vanderbilt University.

[55] Boes, M. K., Islam, M., David Li, Y., & Hsiao-Wecksler, E. T. (2013, June). Fuel efficiency of a portable powered ankle-foot orthosis. In *2013 IEEE 13th International Conference on Rehabilitation Robotics (ICORR),* IEEE.

[56] Frantz, R. A., & Xakellis, G. C. (1989). Characteristics of skin blood flow over the trochanter under constant, prolonged pressure. *American Journal of Physical Medicine & Rehabilitation, 68*(6), 272-276.

[57] What do the compression levels really mean? Retrieved from https://compressionsocks.pro/learn/about-compression.

[58] van Bemmelen, P. S., Mattos, M. A., Faught, W. E., Mansour, M. A., Barkmeier, L. D., Hodgson, K. J., Ramsey, D. E., & Sumner, D. S. (1994). Augmentation of blood flow in limbs with occlusive arterial disease by intermittent calf compression. *Journal of Vascular Surgery, 19*(6), 1052-1058.

[60] Schnorenberg, A. J., Slavens, B. A., Wang, M., Vogel, L. C., Smith, P. A., & Harris, G. F. (2014). Biomechanical model for evaluation of pediatric upper extremity joint dynamics during wheelchair mobility. *Journal of Biomechanics, 47*(1), 269-276.

[61] Borg, G. A. (1982). Psychophysical bases of perceived exertion. *Medicine & Science in Sports & Exercise, 14*(5), 377-381.

[62] Adjusting Your Crutches. Retrieved from http://www.lifebeyond4limbs.com/adjustingyourcrutches/.

[63] Singh, G., Xiao, C., Krishnan, G., & Hsiao-Wecksler, E. T.(2017). *Design and analysis of coiled FREE actuator.* Manuscript submitted for publication.

[64] Xiao, C., Jahanian, O., Schorenberg, A. J., Slavens, B. A., & Hsiao-Wecksler, E. T. (2017, April). Desing and biomechanical evaluation of pneumatic ergonomic crutch. In *2017 Design of Medical Devices Conference*. ASME.

[65] Cramer, D. N., & Barth, E. J. (2013, October). Pneumatic Strain Energy Accumulators for Exhaust Gas Recycling. In ASME/BATH 2013 Symposium on Fluid Power and Motion Control (pp. V001T01A052-V001T01A052). American Society of Mechanical Engineers.

[66] Medline Forearm Crutches. Retrieved from https://www.medline.com/product/Medline-Forearm-Crutches/Forearm-Crutches/Z05-PF04774

[68] Adult Male and Female Height to Weight Ratio Charts. Retrieved from https://www.disabled-world.com/artman/publish/height_weight.shtml

[69] M+D Crutches. Retrieved from https://mobilitydesigned.com/products/set-of-black-m-d-crutches-full-price

[70] Carpal Tunnel Syndrome. Retrieved from https://www.mps1disease.com/en/patients/about/signs-and-symptoms/carpal-tunnel-syndrome.aspx

[71] Carpal Tunnel Syndrome. Retrieved from https://umm.edu/health/medical/reports/articles/carpal-tunnel-syndrome

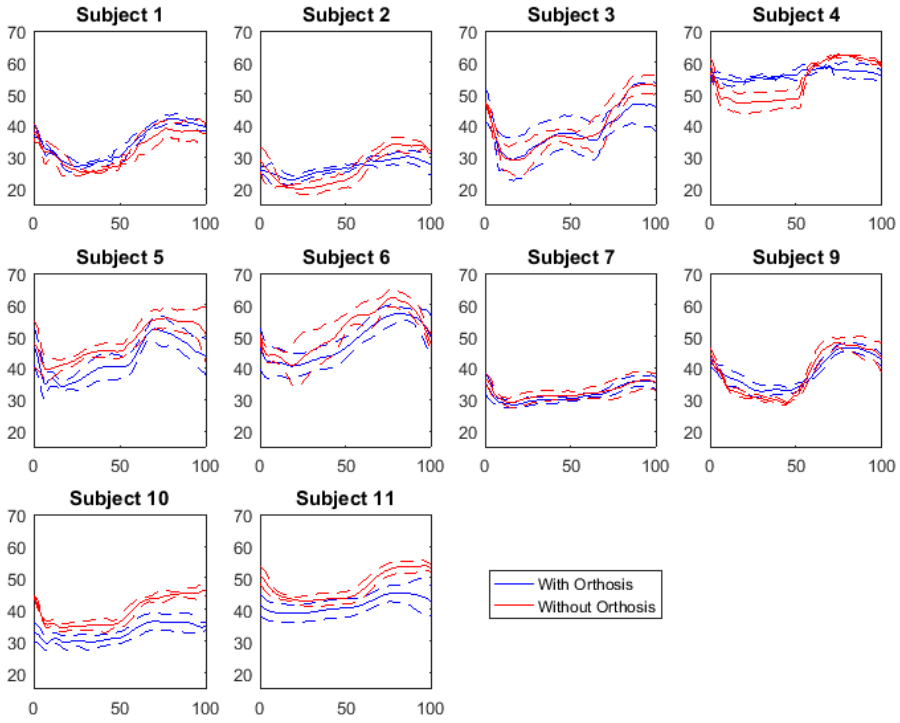

Figure A.1. Wrist extension(+)/flexion(-) angle (deg) vs percentage gait cycle (% Gait) for each subject, swing-through crutch gait

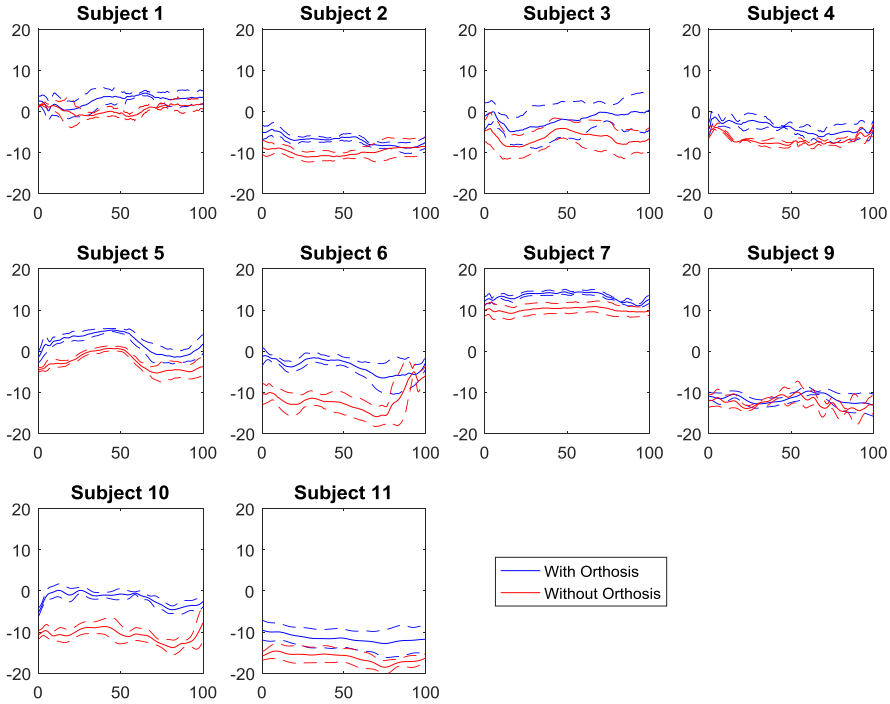

Figure A.2. Wrist radial(+)/ulnar(-) deviation angle (deg) vs percentage gait cycle (% Gait) for each subject, swing-through crutch gait

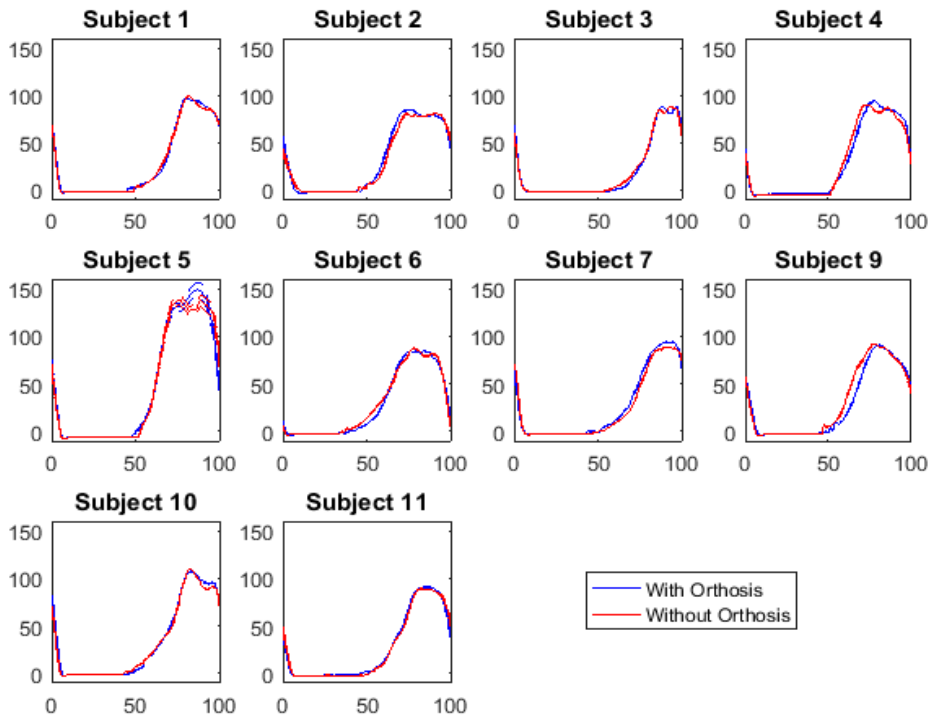

Figure A.3. Averaged normalized crutch shaft force (% BW) vs percentage gait cycle (% Gait) for each subject in swing-through gait

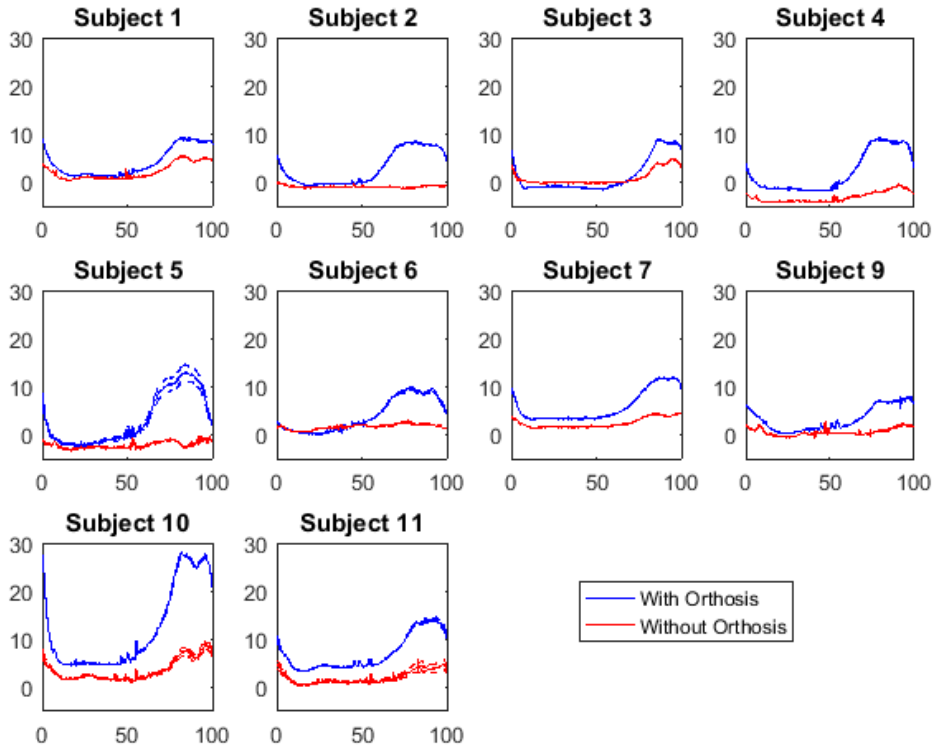

Figure A.4. Averaged normalized crutch cuff force (% BW) vs percentage gait cycle (% Gait) for each subject in swing-through gait

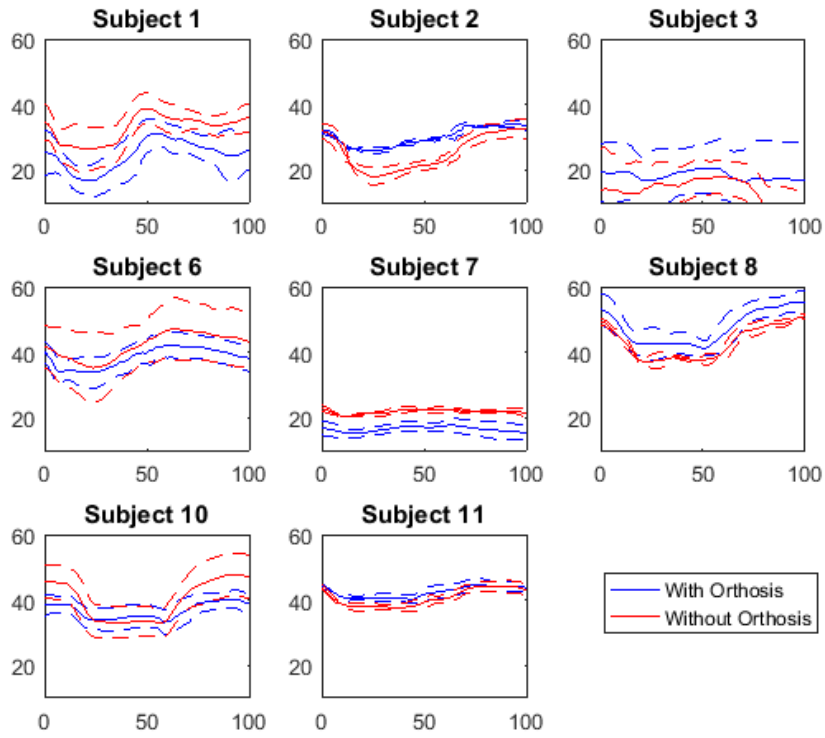

Figure A.5. Wrist extension(+)/flexion(-) angle (deg) vs percentage gait cycle (% Gait) for each subject, reciprocal gait

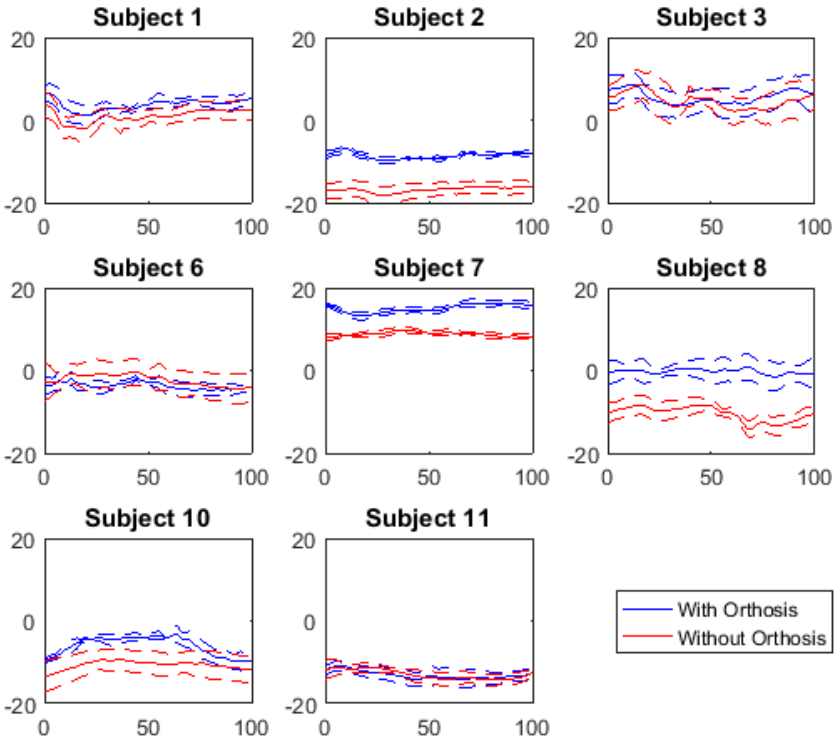

Figure A.6. Wrist radial(+)/ulnar(-) deviation angle (deg) vs percentage gait cycle (% Gait) for each subject, reciprocal gait

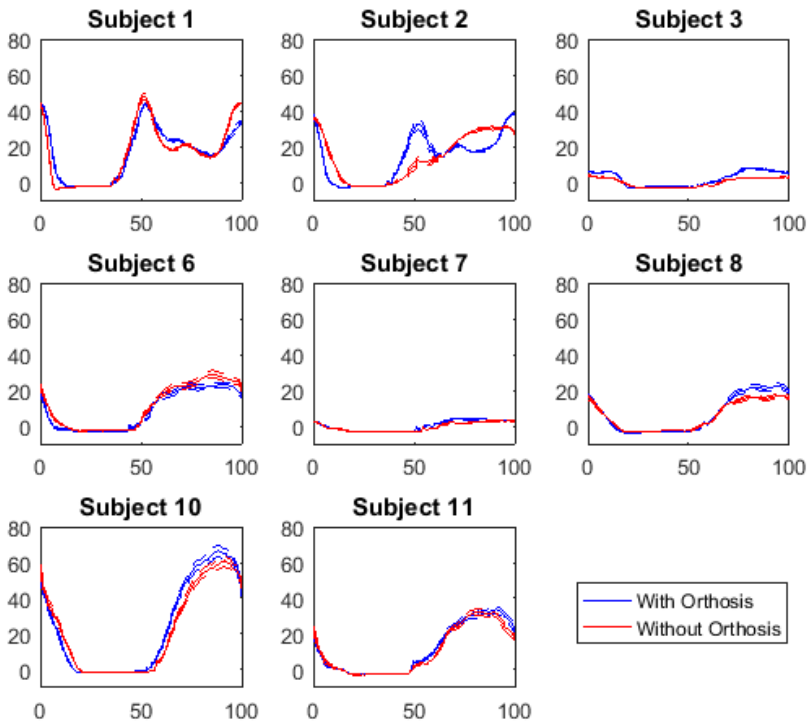

Figure A.7. Averaged normalized crutch shaft force (% BW) vs percentage gait cycle (% Gait) for each subject in reciprocal gait

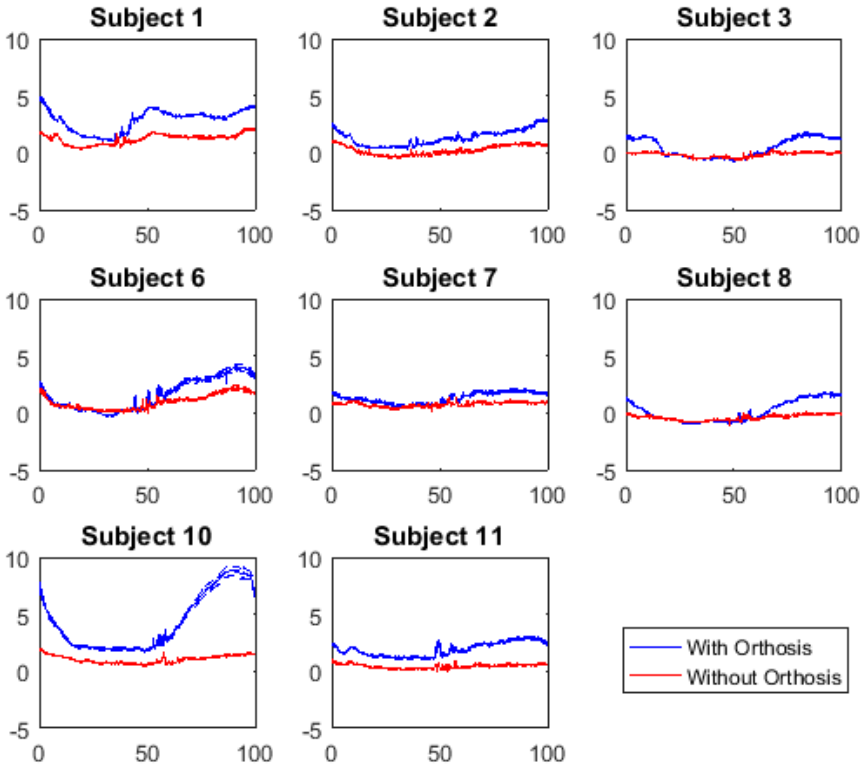

Figure A.8. Averaged normalized crutch cuff force (% BW) vs percentage gait cycle (% Gait) for each subject in reciprocal gait

Table A.1. *Data for swing-through gait trials*

	PEAK Wrist AX (deg)		Mean Wrist AX (deg)		Peak Wrist AZ (deg)	
Subject	With	Without	With	Without	With	Without
1	5.09	3.29	3.50	1.26	-42.74	-40.02
2	9.21	11.55	7.84	9.42	-30.52	-34.55
3	6.93	9.47	2.78	6.37	-48.37	-53.18
4	7.03	8.92	5.07	7.04	-59.38	-62.37
5	5.35	6.11	2.17	3.86	-53.02	-56.29
6	7.26	16.15	5.06	12.02	-57.86	-63.20
7	14.66	10.97	13.06	10.19	-36.92	-37.26
8	8.02	14.31	4.96	12.07	-52.20	-51.28
9	13.73	15.88	11.41	12.85	-46.58	-48.74
10	5.29	13.89	2.72	11.77	-36.90	-46.99
11	13.11	18.75	12.18	17.16	-45.65	-53.99
	ROM Wrist AZ (deg)		Mean Wrist AZ (deg)		Max Palm Pressure (Pa/BW)	
Subject	With	Without	With	Without	With	Without
1	15.99	15.51	-38.76	-35.85	262.79	243.90
2	8.16	14.81	-28.68	-30.83	311.30	316.37
3	19.34	24.67	-41.29	-44.44	365.39	422.51
4	5.89	15.73	-57.34	-59.57	312.02	367.74
5	20.95	18.32	-47.32	-52.89	247.99	282.41
6	17.63	23.64	-53.70	-57.85	507.07	490.81
7	8.80	8.38	-33.30	-33.58	208.50	237.85
8	11.53	13.33	-47.74	-46.35	364.08	346.54
9	14.43	20.05	-42.49	-43.98	515.48	552.79
10	8.41	13.11	-35.06	-43.15	293.54	351.01
11	6.93	11.53	-43.52	-50.53	473.04	604.99
	Mean Palm Pressure (Pa/BW)		Peak Cuff Force (%BW)		Mean Cuff Force (%BW)	
Subject	With	Without	With	Without	With	Without
1	32.72	34.49	9.67	5.93	5.66	2.74
2	51.19	52.75	8.96	0.76	3.62	-1.07
3	22.75	25.79	8.98	5.67	3.07	1.79
4	36.87	40.71	9.76	1.45	4.99	-2.34
5	33.76	38.55	22.43	3.26	12.51	-1.48
6	26.57	43.86	8.95	3.52	3.90	1.00
7	29.14	27.43	10.91	4.49	6.26	2.08
8	39.41	46.30	48.41	16.17	17.46	0.20
9	37.92	44.60	7.96	3.85	3.69	0.24
10	29.14	29.59	24.81	7.03	13.30	1.99
11	36.42	37.23	11.29	3.43	6.55	-0.30

Table A.2. *Data for reciprocal gait trials*

	PEAK Wrist AX (deg)		Mean Wrist AX (deg)		Peak Wrist AZ (deg)	
Subject	With	Without	With	Without	With	Without
1	7.39	5.68	4.39	2.17	-31.52	-38.87
2	10.16	18.31	8.49	16.45	-34.06	-32.96
3	9.88	10.88	5.67	4.55	-23.31	-20.96
6	5.72	5.99	4.24	3.92	-42.52	-47.92
7	16.46	10.07	15.79	8.70	-18.09	-23.37
8	4.24	14.36	2.42	11.90	-55.89	-51.02
10	10.63	13.45	6.53	10.68	-41.04	-48.25
11	14.63	14.73	13.64	13.92	-45.30	-44.69
	ROM Wrist AZ (deg)		Mean Wrist AZ (deg)		Max Palm Pressure (Pa/BW)	
Subject	With	Without	With	Without	With	Without
1	16.35	13.16	-27.56	-35.30	45.84	54.30
2	8.33	15.06	-32.30	-28.22	42.49	54.20
3	10.76	21.46	-17.83	-12.06	11.73	11.42
6	10.84	13.25	-40.79	-45.45	66.55	86.59
7	3.44	3.21	-16.62	-22.02	15.88	16.34
8	15.23	14.70	-50.45	-45.44	43.64	49.74
10	8.82	16.16	-37.50	-42.02	97.28	117.06
11	5.39	7.46	-43.62	-42.63	55.90	64.92
	Mean Palm Pressure (Pa/BW)		Peak Cuff Force (%BW)		Mean Cuff Force (%BW)	
Subject	With	Without	With	Without	With	Without
1	17.35	19.97	5.62	3.62	3.12	1.72
2	18.61	22.94	4.28	2.15	1.93	0.70
3	6.07	4.77	3.07	1.92	0.61	-0.11
6	21.53	23.93	7.17	5.71	3.24	1.97
7	9.01	9.17	5.19	3.89	2.06	1.09
8	20.56	23.24	3.56	2.26	0.95	-0.09
10	21.82	23.97	10.15	3.80	5.88	1.01
11	18.20	22.24	6.55	3.20	2.57	0.24